This work was supported by a Grant-in-Aid for High Technology Research (HTR) from the Ministry of Education, Science, Sports, and Culture, Japan and a Grant-in-Aid for AIDS research from the Ministry of Health, Labor, and Welfare, Japan (H17-AIDS-002)

A

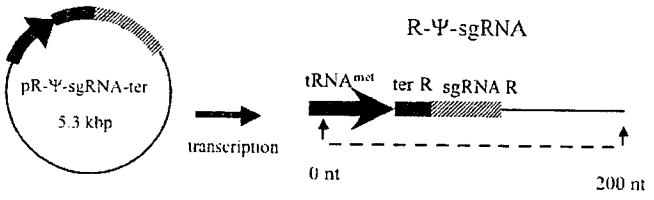

B

5'-GGCAGAACAGCAGAGUGGCGCAGCGGAAGCGUGCUGGGCCCAUAA
CCCAGAGGUCGAUGGAUCGAAACCGGUACCCCAAAAACGUUUGACGC
GUUAUCCAUUGCGCCAAAGGAGACGUACCCGGGGAUCCAGACAUGAU
AAGAUACAUUGAUGAGUUUGGACAAACCACAACUAGAAUGCAGUGAAA
AAAAUGCUUUAUU-3'

Fig1. The RNA expressing from pR-Ψ-sgRNA-ter vector. A. The region of the expressing R-Ψ-sgRNA. tRNA^{met} : tRNA methionine promoter, ter R : reverse sequence of terminator, sgRNA R : reverse sequence of sgRNA B. Sequence of the R-Ψ-sgRNA.

REFERENCES

1. Habu,Y. et al., (2005) NAR, **33**, 235-243.
2. Nashimoto, M (1995) NAR, **23**, 3642-3647.
3. Takaku, H. et al., (2003) NAR, **31**, 2272-2278.

Induction of Natural Killer Cell-dependent Antitumor Immunity by the *Autographa californica* Multiple Nuclear Polyhedrosis Virus

Masayuki Kitajima[1,2], Takayuki Abe[1,3], Naoko Miyano-Kurosaki[1,4], Masaru Taniguchi[5], Toshinori Nakayama[2] and Hiroshi Takaku[1,4]

[1]*Department of Life and Environmental Sciences, Chiba Institute of Technology, Narashino, Chiba, Japan;* [2]*Department of Immunology, Graduate School of Medicine, Chiba University, Chiba, Japan;* [3]*Department of Molecular Virology, Research Institute for Microbial Diseases, Osaka University, Suita, Osaka, Japan;* [4]*High Technology Research Center, Chiba Institute of Technology, Narashino, Chiba, Japan;* [5]*Laboratory for Immune Regulation, RIKEN Research Center for Allergy and Immunology, Yokohama, Japan*

Wild-type *Autographa californica* multiple nuclear polyhedrosis virus (AcMNPV) infects a variety of mammalian cell types *in vitro*, but does not replicate in these cells. We investigated the effects of AcMNPV in the induction of the immune response and tumor metastasis in mice. After intravenous injection, AcMNPV was taken up by the liver and spleen, and preferentially infected dendritic cells (DCs) and B cells in the spleen; costimulatory molecules CD40, CD80, and CD86 were upregulated in the DCs. The hepatic mononuclear cells (MNCs) in these animals were highly cytotoxic to natural killer (NK)-sensitive YAC-1 and B16 melanoma cells, but not to NK-resistant EL4 cells. Intravenous injection of AcMNPV-induced NK cell proliferation in the liver and spleen, and enhanced antitumor immunity in mice with B16 liver metastases. Furthermore, such treatment increased the survival of C57BL/6, Jα281$^{-/-}$, and interferon (IFN)-$\gamma^{-/-}$ mice that were previously injected with B16 tumor cells. AcMNPV injection did not enhance the survival of NK cell-depleted mice. Moreover, one AcMNPV treatment effectively prolonged survival in a B16 liver metastasis model, and was equivalent to five treatments with recombinant interleukin-12 (IL-12) protein. These findings suggest that AcMNPV efficiently stimulates NK cell-mediated antitumor immunity.

Received 12 February 2007; accepted 9 June 2007; published online 4 December 2007. doi:10.1038/sj.mt.6300364

INTRODUCTION

The ability of baculoviruses, including *Autographa californica* multiple nuclear polyhedrosis virus (AcMNPV), to infect insect cells has led to their use in multiple protein expression systems[1,2] and as plant insecticides.[3,4] AcMNPV, the genome of which consists of a circular, double-stranded DNA that contains ~130 kilobase pair[5] surrounded by a large envelope, infects a variety of mammalian cell types, with the exception of certain hematopoietic cell lines, although its genome does not replicate or integrate into mammalian chromosomes.[6,7] Recently, the potential use of these viruses as vectors was explored.[8,9] Unfortunately, except in the case of the mouse brain and testes, these viruses are rapidly inactivated by the classical complement pathway following *in vivo* injection.[10–12] While considerable effort has been expended in an attempt to understand the nature of the host immune response to baculovirus, only a few definitive findings have been reported. The virus induces antiviral cytokine production after being injected *in vivo*, resulting in the protection of cells from infection by the vesicular stomatitis and influenza viruses.[13,14] Furthermore, infected hepatocytes stimulate Kupffer cells to produce tumor necrosis factor-α, interleukin (IL)-1α, and IL-1β when these cells are cocultured *in vitro*.[15]

The purpose of this study was to examine the effects of AcMNPV on immune responsiveness in general, and on antitumor immunity in particular, in mice. Intravenously-injected AcMNPV-infected splenic dendritic cells (DCs) and B cells, increased the percentage of liver mononuclear cells (MNCs) that exhibited natural killer (NK) cell activity, and increased serum interferon (IFN)-γ levels. In liver metastasis models, AcMNPV-induced Vα14 NKT cell-independent and IFN-γ-independent antitumor effects. These results indicate that AcMNPV might be a useful adjunct in the design of antiviral and antitumor therapies.

RESULTS

In vivo infectivity of AcMNPV in B6 mice

Although complement-resistant baculovirus can express inserted foreign genes *in vivo*,[10,16] wild-type (complement-sensitive) baculovirus does not express inserted foreign genes *in vivo*. The tissue tropism of AcMNPV was examined by analyzing total DNA isolated from tissues in B6 mice intravenously-injected with AcMNPV [1×10^8 plaque forming units (PFU)] by means of the polymerase chain reaction (PCR) analysis, using AcMNPV-gp64 specific primers. The AcMNPV titer was based on producing an innate immune response and virus protection in a mouse model by intranasal, intramuscular, intradermal, and intraperitoneal injection.[13] The PCR products of the *gp64* gene were predominantly detected in the liver and spleen following AcMNPV injection; no gp64 PCR

Correspondence: Hiroshi Takaku, Department of Life and Environmental Sciences, Chiba Institute of Technology, 2-17-1 Tsudanuma, Narashino, Chiba 275-0016, Japan. E-mail: hiroshi.takaku@it-chiba.ac.jp

products were detected following vehicle injection (**Figure 1a**). A thin band of gp64 was also detected in the lung, which was likely infected by the pulmonary circulation. This finding suggests that the AcMNPV genome is contained in spleen-accumulated lymphocytes; therefore, we investigated whether AcMNPV infects various lymphocytes in the spleen. The splenocytes were stained with lineage markers CD3 (T, NKT cells), NK1.1 (NK, NKT cells), CD11c (DCs), and CD45R (B cells), and sorted by a cell sorter. AcMNPV-infected cells were examined by PCR using total DNA isolated from sorted cells with AcMNPV-specific primers. AcMNPV-specific bands were detected in total splenocytes and in the $CD3^-$ $NK1.1^-$ population. Total DNA from the T, NK, and NKT cells did not contain the AcMNPV genome (**Figure 1b**). These results indicate that AcMNPV did not infect T, NK, and NKT cells. AcMNPV-specific bands were present in DCs and B cells. The PCR analysis of total DNA from a $CD11c^-$ $CD45R^-$ population failed to amplify the AcMNPV genome (**Figure 1c**). These results suggested that in AcMNPV-injected mice, DCs and B cells as antigen-presenting cells are predominantly infected in the spleen *in vivo*.

We evaluated surface markers for activation on infected $CD11c^+$ DCs by flow-cytometric analysis. Mice were injected intravenously with AcMNPV (1×10^8 PFU) or vehicle, and splenocytes were isolated 24 hours later. We then compared the DC phenotype from AcMNPV-infected and control mice. The mean florescence intensity of costimulatory molecules on infected $CD11c^+$ DCs significantly increased with CD40 (threefold), CD80 (fourfold), and CD86 (16-fold) compared with control $CD11c^+$ DCs (**Figure 1d**), and returned to baseline after 72 hours (data not shown). Costimulatory molecules CD40, CD80, and CD86 were upregulated in $CD11c^+$ DC phenotypes in AcMNPV-treated mice. This result demonstrates that AcMNPV injection activates $CD11c^+$ DCs in mice, thus suggesting that AcMNPV induces an immune response (*i.e.*, DC activation) by infecting DCs and B cells in the spleen and presumably the liver.

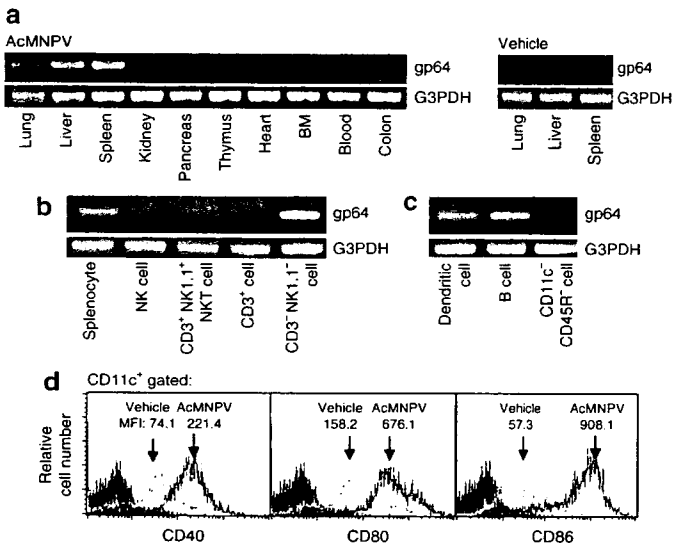

Figure 1 *In vivo Autographa californica* multiple nuclear polyhedrosis virus (AcMNPV) infectivity. (**a**) Mice were injected with AcMNPV [10^8 plaque forming units (PFU)] or vehicle. After 24 hours, the tissues were harvested and total DNA was isolated. The presence of the AcMNPV genome was determined by polymerase chain reaction (PCR) using AcMNPV-gp64 specific primers. The data shown are from duplicate experiments that gave similar results. (**b, c**) Mice were injected with AcMNPV (10^8 PFU), and their splenocytes were harvested 6 hours later and sorted by fluorescence-activated cell sorting. AcMNPV genomic DNA was detected in the lymphocyte total DNA by PCR using specific primers. (**d**) Mice were injected intravenously with AcMNPV (10^8 PFU) or vehicle (phosphate-buffered saline). Splenocytes were isolated and examined by flow cytometry for gated CD11c (fluorescein isothiocyanate), and the activation markers CD40 [phycoerythrin (PE)], CD80 (PE), and CD86 (PE) 24 hours after AcMNPV injection. The mean fluorescence intensity (MFI) is depicted in each panel. The data shown are from duplicate experiments that gave similar results. G3PDH, glyceraldehyde-3-phosphate dehydrogenase; NK cell, natural killer cell.

Effects of AcMNPV on IFN-γ production by lymphocytes

The Th1 immune response has both antiviral and antitumor effects, and is considered to be powerfully induced by the cytokine IFN-γ. The effect of AcMNPV stimulation on IFN-γ levels in mouse serum was investigated. Mice were injected intravenously with AcMNPV (1×10^8 PFU). The serum IFN-γ concentration increased after approximately 3 hours and peaked at 6 hours, returning to baseline levels after 24 hours (**Table 1**). The serum IFN-γ concentration was a function of the AcMNPV titer used (data not shown). The vehicle (phosphate-buffered saline or PBS) injection failed to induce detectable levels of IFN-γ under all the conditions tested. By contrast, IL-12p70 levels in the AcMNPV-treated animals were not significantly different from those in the PBS-injected control animals (data not shown).

To investigate the cytokine expression in AcMNPV-infected tissues, the mRNA levels of inflammatory cytokines (IFN-γ and IL-12p40) were examined in the spleen and liver 2 hours after AcMNPV or vehicle injection using reverse transcription (RT)-PCR methods (**Figure 2a**). We detected IFN-γ and IL-12p40 in the mRNA of the spleen and liver, but not the serum, from AcMNPV-injected mice. The antiviral cytokines IFN-α and IFN-β were also detected using the RT-PCR method (data not shown). The effect of AcMNPV stimulation on *in vivo* tissue lymphocyte IFN-γ production was assessed. AcMNPV stimulation significantly increased the amount of IFN-γ released by both splenocytes and liver MNCs (**Figure 2b**). The increase in IFN-γ released by liver MNCs was approximately sevenfold greater than that released by splenocytes.

Table 1 Effect of AcMNPV on serum concentration of IFN-γ in B6 mice[a]

Treatment	Time (h)	IFN-γ (ng/ml)
Vehicle	6	<0.1
AcMNPV	1	<0.1
	3	1.48 ± 0.2
	6	7.37 ± 2.84
	12	6.24 ± 1.77
	24	<0.1

[a]Mice were injected intravenously with *Autographa californica* multiple nuclear polyhedrosis virus (AcMNPV) (10^8 plaque forming units) or vehicle (phosphate-buffered saline). The concentrations of interferon-γ (IFN-γ) in the sera of mice sacrificed at the times indicated following the injection of AcMNPV were determined by an enzyme-linked immunosorbent assay. Data are the mean ± SD of four mice.

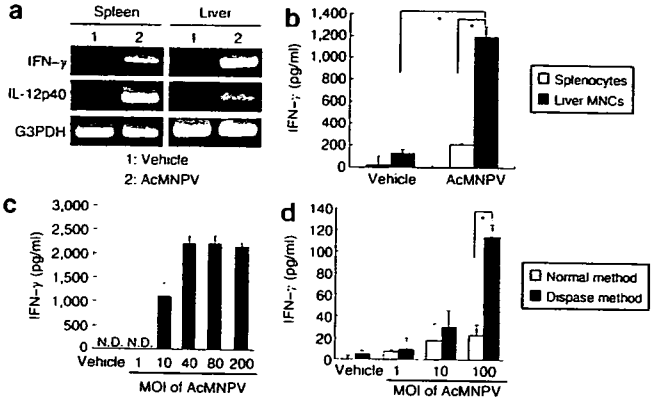

Figure 2 Effect of *Autographa californica* multiple nuclear polyhedrosis virus (AcMNPV) on interferon-γ (IFN-γ) production by splenocytes and liver mononuclear cells (MNCs) *in vivo* and *in vitro*. (**a**) Expression of various cytokine messenger RNAs (mRNAs) in the liver and spleen was detected 2 hours after mice were injected with AcMNPV (10^8 plaque forming units). mRNA expression was determined by reverse transcription polymerase chain reaction using the primers described in the Materials and Methods. The data shown are from duplicate experiments that gave similar results. (**b**) Concentrations of IFN-γ, as determined by enzyme-linked immunosorbent assay (ELISA), in the supernatants of 2-day-old cultures containing splenocytes and liver MNCs that were isolated from mice 6 hours after they were treated with AcMNPV. Data are the mean values ± SEM; $P < 0.01$. (**c**) Production of IFN-γ by splenocytes stimulated *in vitro* with AcMNPV at the indicated multiplicities of infection (MOIs) for 72 hours, as determined by ELISA. The data represent the means ± SEM. Similar results were obtained in two independent experiments. (**d**) Production of IFN-γ by liver MNCs, isolated with or without dispase, that were treated *in vitro* with AcMNPV at the indicated MOIs for 72 hours, as determined by ELISA. The data are the means ± SEM; $^*P < 0.01$. Similar results were obtained in two separate experiments. G3PDH, glyceraldehyde-3-phosphate dehydrogenase; N.D., not detectable.

To examine IFN-γ production *in vitro*, the levels in the supernatants of cultured AcMNPV-stimulated splenocytes were measured by an enzyme-linked immunosorbent assay. IFN-γ production increased as a function of the AcMNPV titer (**Figure 2c**), reaching a plateau at a multiplicity of infection of 40, and remaining constant up to a multiplicity of infection of 200. Microscopic examination of stimulated splenocytes revealed cell aggregation (data not shown). Although *in vitro* AcMNPV stimulation increased IFN-γ levels in the supernatants of stimulated splenocytes, there was no detectable response in the supernatants of stimulated liver MNCs. We therefore compared the responses of liver MNCs, isolated with or without dispase to obtain the Kupffer cells, and found that substantially more IFN-γ was released by the cells isolated with dispase than from those isolated without dispase (**Figure 2d**). This result suggests that liver IFN-γ production in response to AcMNPV infection requires the release of inflammatory cytokines from virus-responsive lymphocytes (*i.e.*, Kupffer cells and/or hepatocytes), and that AcMNPV injection in mice induces IFN-γ production, which is known to have antiviral and antitumor effects.

Induction of NK cell activity by AcMNPV injection

We next examined the cytotoxicity of liver MNCs from AcMNPV-injected B6 mice on YAC-1 (NK-sensitive), EL4 (NK-resistant), and B16 (melanoma) cell lines. B6 mice were sacrificed 48 hours after AcMNPV injection and the cytotoxicity of their liver MNCs

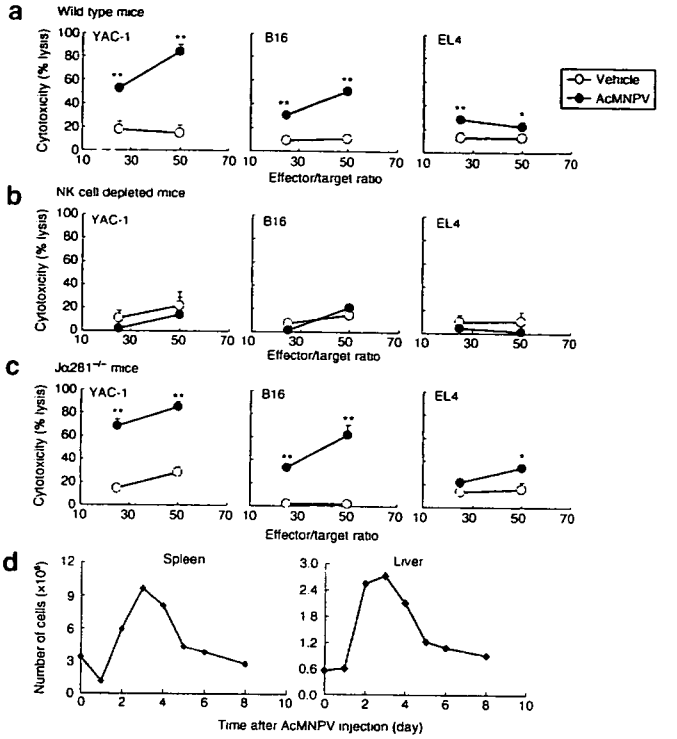

Figure 3 Effect of *Autographa californica* multiple nuclear polyhedrosis virus (AcMNPV) injection on cytotoxic activity and number of natural killer (NK) cells. (**a**) Cytotoxic activity of liver mononuclear cells (MNCs) from AcMNPV-treated or vehicle-treated mice against YAC-1, EL4, and B16 melanoma cells. (**b**) Cytotoxic activity of liver MNCs derived from mice that were pretreated with anti-asialoGM1 antibody before AcMNPV injection. (**c**) Cytotoxic activity of liver MNCs from $J\alpha281^{-/-}$ mice treated with AcMNPV or vehicle. The data are the means ± SD; $^*P < 0.05$; $^{**}P < 0.01$. Similar results were obtained in two separate experiments. (**d**) Numbers of NK cells (FITC-CD3$^-$, PE-NK1.1$^+$) in the spleen and liver of B6 mice on successive days following intravenous injection with AcMNPV, as calculated from flow cytometric data. Similar results were obtained in two independent experiments. FITC, fluorescein isothiocyanate; PE, phycoerythrin.

was tested. Cytotoxicity against YAC-1 and B16 cells increased (**Figure 3a**), whereas there was only minimal cytotoxicity against EL4 cells. AcMNPV injection of B6 mice, but not NK-depleted mice, produced by asialoGM1 injection (**Figure 3b**), increased the cytotoxicity against YAC-1 and B16 cells. Both IL-12 and α-galactosylceramide exert strong antimetastatic effects by inducing Vα14 NKT cell-mediated IFN-γ production and NK cell activation.[17-19] Therefore, we examined the cytotoxicity against YAC-1, EL4, and B16 cells using $J\alpha281^{-/-}$ mice, which were devoid of Vα14 NKT cells while having other lymphoid cell lineages intact, to determine whether AcMNPV induces cytotoxicity in Vα14Jα281 NKT cells. In $J\alpha281^{-/-}$ mice, the cytotoxicity against YAC-1, EL4, and B16 cells was similar to that in B6 mice (**Figure 3c**). Thus, the cytotoxicity of liver MNCs in response to AcMNPV depended on NK cells, but not NKT cells or other immune cells.

Moreover, to examine NK cell activation, we analyzed the time course of the number of CD3$^-$NK1.1$^+$ NK cells in the spleens and livers of B6 mice injected with AcMNPV (1×10^8 PFU) by flow cytometry and cell counting. There was a threefold to fourfold increase in the number of NK cells in the two organs that peaked at 3 days and returned to normal levels after 8 days (**Figure 3d**).

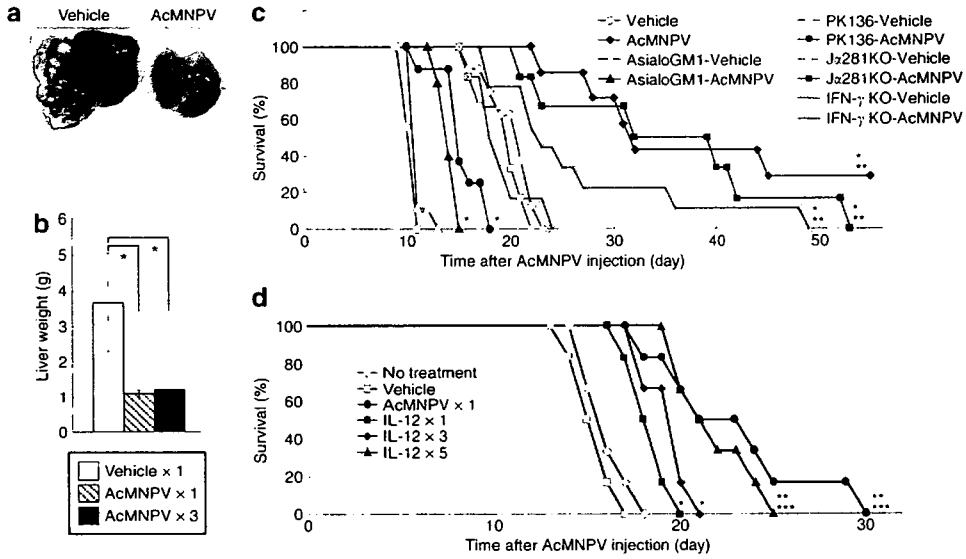

Figure 4 Effect of *Autographa californica* multiple nuclear polyhedrosis virus (AcMNPV) injection on B16 melanoma liver metastases in mice. Mice were injected intrasplenically on day 1 with 1 × 10^6 B16 cells in 0.1 ml phosphate-buffered saline (PBS). (**a**) Representative photographs of the livers of B6 mice on day 14 after they were treated with either vehicle or AcMNPV, showing typical metastases. (**b**) Liver weights of B16 melanoma cell-injected mice (eight per group) that were treated once with vehicle or AcMNPV (day 1), or three times with AcMNPV (days 1, 3, and 7). The data are the means ± SD; $^*P < 0.05$. (**c**) Survival rates of B6 mice that were injected with B16 melanoma cells, some of which were pretreated with anti-asialoGM1 antibody (Ab) (AsialoGM1) or anti-NK1.1 monoclonal Ab (PK136) to deplete them of natural killer (NK) cells or NK and NKT cells, respectively. Survival rates for Jα281$^{-/-}$ and IFN-γ$^{-/-}$ mice that were injected with B16 melanoma cells. $^*P < 0.05$ versus each vehicle-treated group. **Not significant according to the log-rank test. All groups contained between 6 and 11 mice. (**d**) Comparison of antitumor immunity induced by AcMNPV or interleukin-12 (IL-12) in B6 mice. Mice were injected intrasplenically on day 0 with 3 × 10^6 B16 cells in 0.1 ml PBS. Survival rates of B16 melanoma cell-injected mice with no treatment, or those treated with AcMNPV (day 1), vehicle (day 1), or IL-12 (day 1; days 1, 3, and 5; or days 1, 3, 5, 7, and 9). $^*P < 0.05$; $^{**}P < 0.01$. ***Not significant according to the log-rank test. All groups contained six mice.

Moreover, NK cell numbers were similarly increased in the bone marrow and thymus of AcMNPV-treated mice (data not shown). This result indicates that liver and spleen NK cells are activated by AcMNPV injection in mice.

Treating liver metastatic mice with AcMNPV induces NK cell-dependent antitumor immunity

The antiliver metastatic effects of AcMNPV were assessed as follows. Mice were injected intrasplenically on day 0 with 1 × 10^6 B16 cells in 0.1 ml PBS. This was followed by intravenous injection of either AcMNPV (1 × 10^8 PFU) or vehicle on day 1. The mice were killed after day 14. **Figure 4a** shows the typical appearance of the livers at this time. Multiple tumor nodules were clearly visible on the livers of mice that received only vehicle (PBS), in marked contrast to those that received AcMNPV on day 1, which appeared normal. The degree of the antimetastatic effect was measured by weighing the livers. Livers of the AcMNPV-injected mice weighed significantly less than vehicle-injected mice (**Figure 4b**), and were comparable in weight to those of normal mice (~1 g). Tumor development was also inhibited in the livers of the mice that received three AcMNPV injections on days 1, 3, and 7, which did not induce toxicity or tumor growth (**Figure 4b**).

We then evaluated mouse survival rates after intrasplenic injection of B16 cells. This was followed by intravenous injection of either AcMNPV (1 × 10^8 PFU) or vehicle on day 1. Vehicle and AcMNPV injection had comparable effects on survival in wild-type, NK cell-depleted (anti-asialoGM1-treated), and NK/NKT cell-depleted (anti-NK1.1 monoclonal antibody–treated) mice. We confirmed that the antibody-induced depletion of NK cells or NK/NKT cells was maintained for at least 3 days (data not shown). Animals in negative control groups that were pretreated with vehicle, and NK cell-depleted and NKT cell-depleted groups developed rapidly growing tumors that led to the death of the animals within 22 days (**Figure 4c**). By contrast, AcMNPV-treated wild-type mice had a significantly increased survival rate. The survival rates of Jα281$^{-/-}$ or IFN-γ$^{-/-}$ mice were evaluated after intrasplenic injection of B16 cells to determine whether the AcMNPV-induced antimetastatic effects are dependent on Vα14 NKT cells or IFN-γ. AcMNPV, but not vehicle, injection induced antimetastatic effects in Jα281$^{-/-}$ and IFN-γ$^{-/-}$ mice, and the survival rates were similar to those of wild-type mice. These findings suggest that AcMNPV injection induces Vα14 NKT cell-independent and IFN-γ-independent NK cell cytotoxicity against tumor cells in mice.

Comparison of AcMNPV or IL-12-induced antitumor immunity

Cui and colleagues, and Nakagawa and co-workers, suggested that IL-12 and α-galactosylceramide induce antimetastatic effects by activating Vα14Jα281 NKT cells.[18,20] To assess the effects of AcMNPV-induced antitumor immunity, we compared the antimetastatic effects by evaluating differences in survival rate following AcMNPV and recombinant IL-12 protein injections. The appropriate AcMNPV titer was determined for these experimental conditions (**Supplementary Figure S1**). This was accomplished by intravenous injection of either AcMNPV (1 × 10^8 PFU) or vehicle on day 1, and by intraperitoneal injection of recombinant IL-12 protein (1 μg) on days 1; 1, 3, and 5; or 1, 3, 5, 7, and 9.[20]

Here, a more malignant liver metastasis model was produced by increasing the number of injected B16 melanoma cells threefold to investigate the precise difference in the antimetastatic effects. One AcMNPV treatment induced similar survival compared to five recombinant IL-12 treatments (**Figure 4d**). These results suggest that the antimetastatic effects of one AcMNPV and five recombinant IL-12 protein treatments are equally efficient.

Analysis of AcMNPV-induced IFN-γ-independent antitumor immunity

IFN-γ is very important for the induction of cytotoxicity in liver MNCs in α-galactosylceramide-treated mice.[19] We have established mouse survival rates after intrasplenic injection of B16 cells in IFN-$\gamma^{-/-}$ mice (**Figure 4c**). The survival rate in IFN-$\gamma^{-/-}$ mice was clearly increased due to the the AcMNPV injection, but not due to the vehicle injection. We then evaluated the antimetastatic effects mediated by AcMNPV by examining the liver weight of IFN-$\gamma^{-/-}$ mice that were intrasplenically injected with B16 cells as described above. The antimetastatic effects of AcMNPV were assessed in mice that were injected intrasplenically on day 0 with 1×10^6 B16 cells, and with intravenous AcMNPV (1×10^8 PFU/mouse) or vehicle alone on day 1; **Figure 5a** shows the typical appearance of the liver on day 14 in these animals. The antimetastatic effect of AcMNPV was quantified by measuring liver weight, and the results indicated that the mean weight of the livers from AcMNPV-treated mice was significantly lower than that of mice with metastases (**Figure 5b**), and comparable to that in normal mice (~1 g), although a few tumor nodules were present in untreated mice, and this result was similar to the number of liver nodules and liver weight (**Figure 4c**).

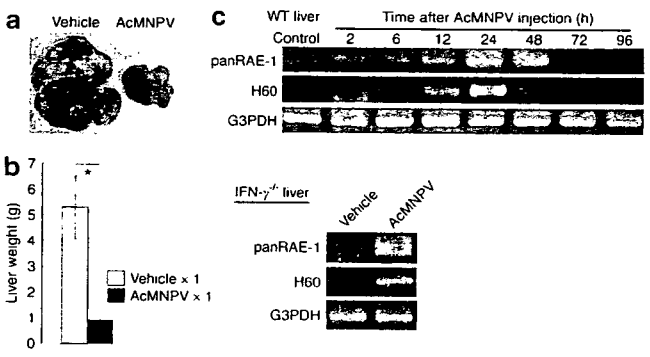

Figure 5 Analysis of antitumor mechanism of *Autographa californica* multiple nuclear polyhedrosis virus (AcMNPV) injection in mice. Mice were injected intrasplenically on day 0 with 1×10^6 B16 cells in 0.1 ml phosphate-buffered saline. (**a**) Representative photographs of the livers from interferon (IFN)-$\gamma^{-/-}$ mice on day 14 after they were treated with either vehicle or AcMNPV, showing typical metastases. (**b**) Liver weights of B16 melanoma cell-injected IFN-$\gamma^{-/-}$ mice (six mice per group) that were treated once with vehicle or AcMNPV (day 1). The data are the means ± SD; $^*P < 0.05$. (**c**) Kinetics of panRAE-1 and H60 messenger RNA (mRNA) expression in the liver induced by AcMNPV injection. mRNA expression was determined by reverse transcription polymerase chain reaction (RT-PCR) using the appropriate specific primers. The data shown are from duplicate experiments that gave similar results. IFN-$\gamma^{-/-}$ mice were injected with AcMNPV or vehicle and their livers were harvested 24 hours later. panRAE-1 and H60 mRNA were detected in the total RNA of their tissues by RT-PCR. The data shown are from duplicate experiments that gave similar results. G3PDH, glyceraldehyde-3-phosphate dehydrogenase; WT liver, wild-type liver.

We demonstrated that AcMNPV, but not vehicle, injection induced antimetastatic effects in IFN-$\gamma^{-/-}$ mice. These findings suggest that AcMNPV-induced IFN-γ-independent NK cell cytotoxicity against tumor cells in mice.

Diefenbach and co-workers reported that the NKG2D ligand, but not cytokine-activated NK cells, inhibits tumor growth.[21] It was possible that IFN-γ independent activation of NK cells by AcMNPV involves the NKG2D ligand, and we therefore examined the expression of NKG2D ligands in the liver of AcMNPV-treated mice by means of RT-PCR. Expression of the NKG2D ligands panRAE-1 and H60 mRNA was detected in total liver RNA of AcMNPV-treated mice, but not in vehicle-treated mice; expression peaked at 24 hours and returned to normal levels after 72 hours (**Figure 5c**). Expression of NKG2D ligands panRAE-1 and H60 mRNA was detected in total liver RNA of AcMNPV-injected IFN-$\gamma^{-/-}$ mice (**Figure 5c**). The data suggest that liver NK cells are IFN-γ-independently activated by the NKG2D ligands Rae-1 and H60 by injection of AcMNPV.

DISCUSSION

Insects are natural hosts for the baculovirus AcMNPV, which is widely used as a pesticide and is considered harmless to humans. Because insects coevolved with humans, it is likely that humans can also produce an efficient immune response against AcMNPV. Mice are unlikely to be naturally infected, but artificial infection with high titers (as used in our experiments) is expected to induce an antiviral (or antitumor) response.

It was previously reported that a recombinant AcMNPV containing a mammalian expression cassette failed to be expressed in immunocompetent recipient animals, and it was suggested that this might be due to viral inactivation by complement protein, an effect that was demonstrated both *in vivo* and *in vitro*.[10,16] These data notwithstanding, in the present study, the virus infected cells in the liver and spleen of immunocompetent C57BL/6 mice (**Figure 1a**). Our results suggest that injection of a high titer of AcMNPV might exceed the ability of the complement to neutralize the virus or, alternatively, that the virus has a high infectivity rate in the liver and spleen. Cheng and colleagues reported that AcMNPV efficiently transduced a variety of adherent, but not suspension, cell lines *in vitro*.[22,23] Wild-type AcMNPV-infected primary suspensions of mouse DCs and B cells *in vivo* (**Figure 1b** and **c**). Such infectivity is thought to result from endocytosis mediated by either DC complement receptors or pathogen-specific Toll-like receptor-recognition of the pathogen components, and by subsequently upregulating costimulatory molecules on DCs (**Figure 1d**). These data suggest that AcMNPV-induced immune activation and infected DCs and B cells in spleen and liver and, together with previous findings, indicate that it is safe to use as a vector in mammals.[24] Our results also suggest, however, that AcMNPV, when present in high titers, is recognized as a pathogen by DCs, and induces a DC-activated immune response in mice.

Baculovirus is rapidly inactivated by the classical complement pathway following in *vivo* injection.[10,11] We demonstrate that intravenous injection of AcMNPV induces IFN-γ production in serum (**Table 1**). The increased production of IFN-γ by liver MNCs compared to splenocytes that was stimulated *in vivo* with AcMNPV (**Figure 2a** and **b**) might have been due to the fact that

intravenously injected substances tend to accumulate in the liver (**Figure 1a**). *In vitro* AcMNPV stimulation, however, induced lower IFN-γ levels in the liver than in splenocytes (**Figure 2d**). The results described above suggest that intravenously-injected AcMNPV is inactivated by the classical complement cascade in serum, after which it is clearly excluded by IFN-γ-producing hepatic MNCs that are activated by inflammatory cytokines produced by activated Kupffer cells, and/or hepatocytes activated by AcMNPV stimulation.[15] Moreover, this result suggests that IFN-γ production in liver MNCs following AcMNPV stimulation requires other factors in the blood or liver. We assumed that AcMNPV might also induce strong antitumor and antiviral Th1 responses that are mediated, at least in part, by IFN-γ.

Nakagawa and co-workers, and Smyth and colleagues, suggested that IL-12 and α-galactosylceramide induce IFN-γ production by Vα14Jα281 NKT cells, and that NK cells have antimetastatic effects in the liver.[20,25] Initially, we provided evidence for strong AcMNPV-induced cytotoxic activity of liver MNCs against NK cell-sensitive YAC-1 and B16 melanoma cell lines, but not against the NK-resistant EL4 cell line, using B6 (**Figure 3a**). AcMNPV-induced cytotoxicity disappeared in NK cell-depleted mice (**Figure 3b**), but not in Jα281$^{-/-}$ mice (**Figure 3c**). In fact, AcMNPV injection increased the NK cell number in the liver and spleen (**Figure 3d**). Our results demonstrate that AcMNPV injection induces NK cell activation, and augments NK cell-dependent, Vα14 NKT cell-independent, cytotoxicity. NK cells in AcMNPV-treated mice were not infected (**Figure 1b**); therefore, these data suggest that NK cell activation mediates antigen-presenting cells because AcMNPV infects DCs.

Wild-type mice treated with AcMNPV had a significantly increased survival rate in a liver metastasis model (**Figure 4c**). This result is consistent with the finding that liver tumor nodules and liver weight in AcMNPV-treated mice are normal (**Figure 4a** and **b**). A similar antimetastatic effect (tumor nodules) was observed with AcMNPV injection 3 days after B16 injection (data not shown). Furthermore, liver metastasis after repeated AcMNPV injections (days 1, 3, and 7) induced similar antitumor effects without toxicity or tumor growth compared with one injection of AcMNPV (**Figure 4b**). These results demonstrate that repeated AcMNPV injection induces antiliver metastatic effects without toxicity. Vehicle or AcMNPV-treated NK cell or NK/NKT cell-depleted mice died more rapidly than vehicle-treated non-depleted wild-type mice. Treatment with AcMNPV in both NK cell and NK/NKT cell-depleted mice, however, prolonged survival by ~5 days, compared with vehicle-treated NK cell and NK/NKT cell-depleted mice (**Figure 4c**). This increased survival rate indicates that the AcMNPV-induced antimetastasis effects might involve unknown NK cell-independent mechanisms. The survival rate of Jα281$^{-/-}$ and IFN-$\gamma^{-/-}$ mice was similar to that of wild-type mice in AcMNPV-treated and vehicle-treated mice. These results indicate that the antimetastatic effects of AcMNPV-induced NK cell activation differ from the antimetastatic effects of α-galactosylceramide-induced Vα14 NKT cell-dependent NK cell activation. Thus, the AcMNPV-induced antimetastasis effects in mice are NK cell-dependent, and Vα14 NKT cell and IFN-γ-independent.

To assess the strength of AcMNPV-induced antitumor immunity, we compared the antimetastatic effects by measuring differences in survival between a single AcMNPV treatment and five treatments of recombinant IL-12 protein. The antimetastatic effect of AcMNPV was similar to that of recombinant IL-12 protein (**Figure 4d**). Thus, AcMNPV and IL-12 are equally effective in a liver metastasis model; however, the antimetastasis mechanisms for the NK cell-dependent, Vα14 NKT cell-independent, antitumor activity of AcMNPV differ from the Vα14 NKT cell-dependent antitumor activity of IL-12, and might be useful in the development of tumor immunity.

In this study, mRNA expression of the NKG2D ligand H60 and panRAE-1 was detected in the total RNA of livers from both B6 and IFN-$\gamma^{-/-}$ mice injected with AcMNPV (**Figure 5c**). Recently, Diefenbach and colleagues reported that NKG2D ligand, but not cytokine-activated NK cells, significantly inhibit tumor growth.[21] By contrast, Hamerman and co-workers reported that lipopolysaccharides and poly(I;C) activate Toll-like receptor signaling and induce the expression of an NKG2D receptor ligand on macrophages.[26] More recently, T.A. and co-workers reported that AcMNPV was recognized by Toll-like receptor 9 expressed on DCs and macrophages, but heat-inactivated AcMNPV was not recognized.[27] Moreover, adenovirus containing genomic DNA and AcMNPV induces the expression of the NKG2D ligand H60 in mice, and activates NK cells,[28] suggesting that AcMNPV induced IFN-γ-independent cytotoxicity of NK cells by inducing the expression of an NKG2D ligand, such as H60 and Rae-1, on the virus-infected antigen-presenting cells in the liver. A more detailed investigation is needed to clarify this issue.

Insects are the natural hosts of AcMNPV, and the virus is thought to be safe in these organisms. The safety of the virus for applications in human is, however, not known, and toxicity in animals must be examined prior to its use in clinical trials. No activation of hepatic enzymes, such as plasma alanine aminotransferase and aspartate aminotransferase, was observed in serum 3 days after injection into B6 mice with AcMNPV (data not shown). The virus does not replicate in mammals and is not toxic to mammalian cells.[7] Consequently, AcMNPV is clinically used in multiple protein expression systems[5,22] and in plant insecticides, as the baculoviruses have been registered as insecticides with the US Environmental Protection Agency.[3,4] Humans are the hosts of most other viruses used for therapy, which causes various problems, such as replication and toxicity, but humans are not hosts of baculovirus.

In conclusion, AcMNPV predominantly infected antigen-presenting cells, and activated DCs and NK cells in mice. Furthermore, AcMNPV efficiently stimulated NK cell-dependent antitumor immunity, but is Vα14 NKT cell and IFN-γ-independent. Therefore, AcMNPV might be potentially useful in clinical trials as an efficient antimetastatic agent, and is expected to be useful in the development of antitumor therapies.

MATERIALS AND METHODS

Animals and cell lines. Female C57BL/6 (B6) mice were purchased from Nippon SLC (Hamamatsu, Japan). B6.Jα281$^{-/-}$ mice lacking the Jα281 T-cell receptor gene segment, which were devoid of Vα14 NKT cells while having other lymphoid cell lineages intact (hereafter referred to as Jα281$^{-/-}$ mice), were generated as previously described.[17] B6.IFN-$\gamma^{-/-}$ mice were obtained from Yoichiro Iwakura (Tokyo University, Tokyo, Japan). All mice used were between 5 and 10 weeks of age. The

B16 melanoma, YAC-1, and EL4 cell lines were obtained from the Riken Cell Bank (Wako, Japan). B16 melanoma and EL4 cells were maintained in Dulbecco's modified Eagle's medium (Sigma Chemical, St. Louis, MO), and YAC-1 cells were maintained in Rosewell Park Memorial Institute (RPMI) 1640 (Sigma Chemical), both of which were supplemented with 10% fetal bovine serum, 100 U/ml penicillin (Invitrogen, Carlsbad, CA) and 100 μg/ml streptomycin (Invitrogen).

Purified wild-type AcMNPV. Wild-type baculovirus AcMNPV was purchased from BD Bioscience (San Diego, CA). Sf-9 insect cells were cultured at 27 °C in Sf-900IISFM (Invitrogen, Carlsbad, CA) containing 10% fetal bovine serum and 100 μg/ml kanamycin sulfate. Purification of the baculovirus by filtration and the sucrose gradient method was performed as previously described.[29] The virus stocks were endotoxin-free (<0.01 U/ml), as determined using a Pyrodick endotoxin measurement kit (Seikagaku, Tokyo, Japan).

Isolation of liver MNCs and splenocytes. Splenocytes were passed through a nylon mesh, centrifuged, and resuspended in red blood cell lysis solution [1.54 mol/l NH_4Cl, 14 mmol/l $NaHCO_3$, and 0.1 mmol/l $EDTA_2Na$ (pH 7.3)], after which they were washed in PBS and resuspended in RPMI 1640 culture medium. Liver MNCs were prepared as described previously.[30] To obtain liver MNCs with Kupffer cells, the cells were harvested by agitating the liver in RPMI 1640 containing 10% fetal bovine serum and 2 U/ml dispase (Godo Shusei, Tokyo, Japan), which comprises a cocktail of proteolytic enzymes, principally collagenase, and is used for dispersing tissues and cells, at 37 °C, after which they were passed through a nylon mesh. After three washes with RPMI 1640, the cells were resuspended in 33% Percoll solution (Amersham Biosciences, Piscataway, NJ), containing 100 U/ml heparin and centrifuged at 2,000 rpm for 20 minutes at room temperature. Pellets were resuspended in red blood cell lysis solution, washed three times in PBS, and resuspended in culture medium.

PCR and analysis of amplified products. Total DNA was purified from various tissues, and the presence of AcMNPV was detected by performing PCR for the viral gene AcMNPV-gp64. The sequences of the specific primers were as follows: AcMNPV gp64, 5′-CTACTAGTAAATCAGTCACACC-3′ (sense) and 5′-CCAAGTTTTTTAATCTTGTACGG-3′ (antisense); glyceraldehyde-3-phosphate dehydrogenase, 5′-TCCACCACCCTGTTGCTGTA-3′ (sense) and 5′-ACCACAGTCCATGCCATCAC-3′ (antisense).

RT-PCR and analysis of amplified products. Total RNAs were extracted from cells using a GenElute Mammalian Total RNA Miniprep Kit (Sigma Chemical), according to the manufacturer's instructions. One-step RT-PCR was performed on RNA samples by RT-PCR high-Plus- (Toyobo, Osaka, Japan). The sequences of specific primers were as follows: IL-12p40, 5′-TCTGCAGAGAAGGTCACACTGGACCAAAG-3′ (sense) and 5′-ATGCCCACTTGCTGCATGAGGAATT-3′ (antisense); IFN-γ, 5′-ACACACTGCATCTTGGCTTTGCAGCT-3′ (sense) and 5′-GGACCTGTGGGTTGTTGACCTCAAACTT-3′ (antisense); IFN-α, 5′-TGAAGGACAGGAAGGACTTTGGATTCCC-3′ (sense) and 5′-TCTCTCAGTCTTCCCAGCACATTGGCA-3′ (antisense); IFN-β, 5′-TACAGGGCGGACTTCAAGATCCCTATG-3′ (sense) and 5′-CATCCAGGCGTAGCTGTTGTACTTCATG-3′ (antisense); panRAE-1, 5′-GAAGTGGGGGAATGTTTGACACAACC-3′ (sense) and 5′-GGACCTTGAGGTTGATCTTGGCTTTTC-3′ (antisense); and H60, 5′-TCTGGGCCATCAACACTGATGAACAG-3′ (sense) and 5′-CACCAAGCGAATACCATGAATGCCA-3′ (antisense).

Flow cytometry. Surface antigens were labeled with fluorescent monoclonal antibodies according to the protocols provided by BD Bioscience, which supplied all of our reagents. The monoclonal antibodies included fluorescein isothiocyanate conjugated anti-CD3 (17A2), phycoerythrin (PE)-conjugated anti-NK1.1 (PK136), PE-conjugated anti-CD4 (H129.19), PE-conjugated anti-CD8α (53-6.7), PE-conjugated anti-CD45R (RA3-6B2), PE-conjugated anti-CD11b (M1/70), fluorescein isothiocyanate-conjugated anti-CD11c (HL3), PE-conjugated anti-CD40 (GL1), PE-conjugated anti-CD80 (16-10A1), and PE-conjugated anti-CD86 (GL1). Cell subsets were analyzed using a fluorescence-activated cell sorting (FACS) Vantage cell sorter (Becton Dickinson, Mountain View, CA); all of the sorted populations were at least 90% pure.

Cytotoxicity assay. The effector cells in this assay were liver MNCs obtained from mice 48 hours after they had been intravenously-injected with AcMNPV (1×10^8 PFU), and the target cells were either B16 melanoma, YAC-1, or EL4 cells ($0.5–1 \times 10^4$/well). The effector and target cells were coincubated in RPMI 1640 containing 10% fetal bovine serum (total volume of 100 μl) in a 96-well round-bottomed microtiter plate. The cytotoxicity was determined using the CytoTox 96 Non-Radioactive Cytotoxicity Assay kit (Promega, Madison, WI). The spontaneous release from target cells was determined to be less than 10% of the maximum release.

In vivo ***lymphocyte stimulation with baculovirus AcMNPV.*** Six hours after the mice were treated with AcMNPV (1×10^8 PFU/mouse) or vehicle, their lymphocytes were harvested and 5×10^5 cells were cultured in a total volume of 200 μl medium in a 96-well flat-bottomed microtiter plate, at 37 °C in a humidified 5% CO_2 incubator. Forty-eight hours later, the supernatants were harvested and centrifuged, and the IFN-γ concentration was determined using an enzyme-linked immunosorbent assay kit (BD Bioscience).

In vitro ***lymphocyte stimulation with baculovirus AcMNPV.*** Isolated lymphocytes (5×10^5) were cultured in a total volume of 200 μl medium in a 96-well flat-bottomed microtiter plate, at 37 °C in a humidified 5% CO_2 incubator, to which an aliquot of AcMNPV, vehicle (PBS), or control medium (culture medium) was added. Seventy-two hours later, the supernatants were harvested and centrifuged, and the IFN-γ concentration was determined using an enzyme-linked immunosorbent assay kit (BD Bioscience).

In vivo ***depletion of specific immune cells.*** Two or three days before the mice were treated with vehicle or AcMNPV, they were injected intraperitoneally with 50 μl anti-asialoGM1 antiserum (Wako Chemical, Osaka, Japan) or 100 μl ascites fluid from the PK136 hybridoma (anti-NK1.1; American Type Culture Collection). The depletion of NK cells and NK/NKT cells, as assessed by flow cytometry, was >90%.

B16 melanoma model of liver metastases. To induce liver metastases, mice were injected intrasplenically with ~$1–3 \times 10^6$ B16 cells in 0.1 ml PBS. The apertures of the injected spleens were surgically sutured after tying the vessels to arrest the blood flow. On day 1, the mice were intravenously injected with either AcMNPV (1×10^8 PFU/mouse) or vehicle. On day 1, days 1, 3, and 5, or days 1, 3, 5, 7, and 9 after injection of B16 cells, the animals were intravenously-injected with recombinant IL-12 protein (1 μg/mouse; R&D Systems, Minneapolis, MN) or vehicle.[19] Fourteen days later, the mice were sacrificed, and their livers were weighed and examined for visible metastases.

Serum alanine aminotransferase and aspartate aminotransferase. The mice were intravenously-injected with either AcMNPV (1×10^8 PFU/mouse) or vehicle, and serum samples were collected 3 days later. The serum alanine aminotransferase activity and aspartate aminotransferase activity were determined by commercial kits (Wako Pure Chemical Industries, Osaka, Japan).

Statistical analysis. Data were analyzed using a two-tailed Student's *t*-test. The mouse survival rates were analyzed by the log-rank test. A P value <0.05 was considered to be statistically significant.

ACKNOWLEDGMENTS

We thank Yoichiro Iwakura (Tokyo University, Tokyo, Japan) for providing the IFN-$\gamma^{-/-}$ mice. This work was supported, in part, by a Grant-in-Aid for High Technology Research (No. 09309011) from the Ministry

of Education, Science, Sports, and Culture, Japan, and by a grant for Research and Development Program for New Bio-industry Initiatives.

SUPPLEMENTARY MATERIAL

Figure S1. Survival analysis of antitumor effect in titrated AcMNPV injection in mice.

REFERENCES

1. Berger, I, Fitzgerald, DJ and Richmond, TJ (2004) Baculovirus expression system for heterologous multiprotein complexes. *Nat Biotechnol* **22**: 1583–1587.
2. Matsuura, Y, Possee, RD, Overton, HA and Bishop, DH (1987) Baculovirus expression vectors: the requirements for high level expression of proteins, including glycoproteins. *J Gen Virol* **68**: 1233–1250.
3. Jennifer, SC, Mark, LH, Trevor, W, Rosemary, SH, David, G, Bernadette, MG *et al.* (1994) Field trial of a genetically improved baculovirus insecticide. *Nature* **370**: 138–140.
4. Stewart, LM, Hirst, M, López-Ferber, M, Merryweather, AT, Cayley, PJ and Possee, RD (1991) Construction of an improved baculovirus insecticide containing an insect-specific toxin gene. *Nature* **352**: 85–88.
5. Ayres, MD, Howard, SC, Kuzio, J, Lopez-Ferber, M and Possee, RD (1994) The complete DNA sequence of *Autographa californica* nuclear polyhedrosis virus. *Virology* **202**: 586–605.
6. Hofmann, C, Sandig, V, Jennings, G, Rudolph, M, Schlag, P and Strauss, M (1995) Efficient gene transfer into human hepatocytes by baculovirus vectors. *Proc Natl Acad Sci USA* **92**: 10099–10103.
7. Tjia, ST, zu Altenschildesche, GM and Doerfler, W (1983) *Autographa californica* nuclear polyhedrosis virus (AcNPV) DNA does not persist in mass cultures of mammalian cells. *Virology* **125**: 107–117.
8. Song, SU and Boyce, FM (2001) Combination treatment for osteosarcoma with baculoviral vector mediated gene therapy (p53) and chemotherapy (adriamycin). *Exp Mol Med* **33**: 46–53.
9. Ylä-Herttuala, S and Alitalo, K (2003) Gene transfer as a tool to induce therapeutic vascular growth. *Nat Med* **9**: 694–701.
10. Hofmann, C and Strauss, M (1998) Baculovirus-mediated gene transfer in the presence of human serum or blood facilitated by inhibition of the complement system. *Gene Ther* **5**: 531–536.
11. Hüser, A, Rudolph, M and Hofmann, C (2001) Incorporation of decay-accelerating factor into the baculovirus envelope generates complement-resistant gene transfer vectors. *Nat Biotechnol* **19**: 451–455.
12. Tani, H, Limn, CK, Yap, CC, Onishi, M, Nozaki, M, Nishimune, Y *et al.* (2003) *In vitro* and *in vivo* gene delivery by recombinant baculoviruses. *J Virol* **77**: 9799–9808.
13. Abe, T, Takahashi, H, Hamazaki, H, Miyano-Kurosaki, N, Matsuura, Y and Takaku, H (2003) Baculovirus induces an innate immune response and confers protection from lethal influenza virus infection in mice. *J Immunol* **171**: 1133–1139.
14. Gronowski, AM, Hilbert, DM, Sheehan, KC, Garotta, G and Schreiber, RD (1999). Baculovirus stimulates antiviral effects in mammalian cells. *J Virol* **73**: 9944–9951.
15. Beck, NB, Sidhu, JS and Omiecinski, CJ (2000). Baculovirus vectors repress phenobarbital-mediated gene induction and stimulate cytokine expression in primary cultures of rat hepatocytes. *Gene Ther* **7**. 1274–1283.
16. Sandig, V, Hofmann, C, Steinert, S, Jennings, G, Schlag, P and Strauss, M (1996). Gene transfer into hepatocytes and human liver tissue by baculovirus vectors. *Hum Gene Ther* **7**: 1937–1945.
17. Cui, J, Shin, T, Kawano, T, Sato, H, Kondo, E, Toura, I *et al.* (1997). Requirement for Valpha14 NKT cells in IL-12-mediated rejection of tumors. *Science* **278**: 1623–1626.
18. Kawano T, Cui, J, Koezuka, Y, Toura, I, Kaneko, Y, Sato, H *et al.* (1998) Natural killer-like nonspecific tumor cell lysis mediated by specific ligand-activated Valpha14 NKT cells. *Proc Natl Acad Sci USA* **95**: 5690–5693.
19. Nakagawa, R, Motoki, K, Ueno, H, Iijima, R, Nakamura, H, Kobayashi, E *et al.* (1998) Treatment of hepatic metastasis of the colon26 adenocarcinoma with an alpha-galactosylceramide, KRN7000. *Cancer Res* **58**: 1202–1207.
20. Nakagawa, R, Nagafune, I, Tazunoki, Y, Ehara, H, Tomura, H, Iijima, R *et al.* (2001) Mechanisms of the antimetastatic effect in the liver and of the hepatocyte injury induced by alpha-galactosylceramide in mice. *J Immunol* **166**: 6578–6584.
21. Diefenbach, A, Jensen, ER, Jamieson, AM and Raulet, DH (2001) Rae1 and H60 ligands of the NKG2D receptor stimulate tumour immunity. *Nature* **413**: 165–171.
22. Cheng, T, Xu, CY, Wang, YB, Chen, M, Wu, T, Zhang, J *et al.* (2004) A rapid and efficient method to express target genes in mammalian cells by baculovirus. *World J Gastroenterol* **10**: 1612–1618.
23. Condreay, JP, Witherspoon, SM, Clay, WC and Kost, TA (1999) Transient and stable gene expression in mammalian cells transduced with a recombinant baculovirus vector. *Proc Natl Acad Sci USA* **96**: 127–132.
24. Hüser, A and Hofmann, C (2003) Baculovirus vectors: novel mammalian cell gene-delivery vehicles and their applications. *Am J Pharmacogenomic* **3**: 53–63.
25. Smyth, MJ, Cretney, E, Takeda, K, Wiltrout, RH, Sedger, LM, Kayagaki, N *et al.* (2001) Tumor necrosis factor-related apoptosis-inducing ligand (TRAIL) contributes to interferon gamma-dependent natural killer cell protection from tumor metastasis. *J Exp Med* **193**: 661–670.
26. Hamerman, JA, Ogasawara, K and Lanier, LL (2004) Cutting edge: Toll-like receptor signaling in macrophages induces ligands for the NKG2D receptor. *J Immunol* **172**: 2001–2005.
27. Abe, T, Hemmi, H, Miyamoto, H, Moriishi, K, Tamura, S and Takaku, H *et al.* (2005) Involvement of the Toll-like receptor 9 signaling pathway in the induction of innate immunity by baculovirus. *J Virol* **79**: 2847–2858.
28. Peng, Y, Falck-Pedersen, E and Elkon, KB (2001) Variation in adenovirus transgene expression between BALB/c and C57BL/6 mice is associated with differences in interleukin-12 and gamma interferon production and NK cell activation. *J Virol* **75**: 4540–4550.
29. Boyce, FM and Bucher, NL (1996) Baculovirus-mediated gene transfer into mammalian cells. *Proc Natl Acad Sci USA* **93**: 2348–2352.
30. Dobashi, H, Seki, S, Habu, Y, Ohkawa, T, Takeshita, S, Hiraide, H *et al.* (1999) Activation of mouse liver natural killer cells and NK1.1$^+$ T cells by bacterial superantigen-primed Kupffer cells. *Hepatology* **30**: 430–436.

CLINICAL AND VACCINE IMMUNOLOGY, Feb. 2008, p. 376–378 Vol. 15, No. 2
1556-6811/08/$08.00+0 doi:10.1128/CVI.00285-07

NOTES

Induction of Antitumor Acquired Immunity by Baculovirus *Autographa californica* Multiple Nuclear Polyhedrosis Virus Infection in Mice[▽]

Masayuki Kitajima[1,3] and Hiroshi Takaku[1,2]*

Department of Life and Environmental Sciences[1] and High Technology Research Center,[2] Chiba Institute of Technology, 2-17-1 Tsudanuma, Narashino, Chiba 275-0016, Japan, and Department of Immunology, Graduate School of Medicine, Chiba University, 1-8-1 Inohana Chuo-ku, Chiba 260-8670, Japan[3]

Received 9 July 2007/Returned for modification 15 October 2007/Accepted 19 November 2007

The baculovirus *Autographa californica* multiple nuclear polyhedrosis virus (AcMNPV) has been studied as a gene therapy vector. Here, we demonstrated that AcMNPV induces antitumor acquired immunity. These results suggest that AcMNPV has the potential to be an efficient virus or tumor therapy agent which induces innate and acquired immunity.

Autographa californica multiple nuclear polyhedrosis virus (AcMNPV) has a double-stranded circular DNA genome of approximately 130 kb that contains more than 150 open reading frames (4). The ability of AcMNPV to infect insect cells has led to its use in multiple protein expression systems (5, 16) and as plant insecticides (8, 21). AcMNPV also infects a variety of mammalian cell types, with the exception of certain hematopoietic cell lines, although its genome does not replicate or integrate into mammalian chromosomes (9, 11, 13, 17, 23).

Considerable attempts have been made to understand the nature of host immune responses to baculovirus. In vivo studies found that the virus induces antiviral cytokine production, which protects cells from infection with vesicular stomatitis virus and influenza virus (2, 10). Recently, Abe and coworkers demonstrated that AcMNPV is recognized by Toll-like receptor 9 on dendritic cells (DCs) and macrophages (1). More recently, we found that wild-type AcMNPV infects DCs and induces natural killer (NK) cell-dependent antimetastatic effects in mice (12). These results suggest that wild-type AcMNPV induces the activation of NK cells and has the potential for virus or tumor therapy. However, it is not yet known whether such antitumor effects are achieved by the induction of acquired immunity. The purpose of this study, therefore, was to examine wild-type AcMNPV-induced acquired immunity, such as the activation of tumor-specific cytotoxic lymphocytes (CTLs) and antibodies.

To investigate AcMNPV-induced acquired immunity in mice, we used two experimental tumor models: the liver metastasis model and the subcutaneous tumor model. Mice were injected intrasplenically with vehicle, mouse melanoma B16 cells, or hepatocellular carcinoma Hepa1-6 cells (n = 6 to 11) (Fig. 1A). The liver metastasis model was performed as previously described (12). Purified AcMNPV (1×10^8 PFU/mouse) was injected intravenously on day 1. After 2 weeks, mice received a secondary subcutaneous challenge with 2×10^5 B16 cells in 0.1 ml phosphate-buffered saline. Mice were monitored every 2 to 3 days for tumor growth, which was measured with calipers. The tumor volume (mm^3) was calculated (18).

Mice injected with vehicle alone, with AcMNPV alone, or with AcMNPV after intrasplenic delivery of vehicle or Hepa1-6 cells were unable to eradicate the secondary tumor challenge. By contrast, tumor growth was significantly retarded in mice injected with AcMNPV following intrasplenic treatment with B16 cells (Fig. 1B). We demonstrated that no AcMNPV-injected mice in the liver metastasis model survived for 30 days after intrasplenic B16 injection (12). This demonstrates that the AcMNPV-induced antimetastasis effects developed from systematic antitumor acquired immunity toward the first injection of tumor cells.

In acquired immunity, CTLs have a very important role (3, 14), and many studies have investigated their antitumor effects. Here, we examined whether tumor-specific CTL cytotoxicity was induced by AcMNPV treatment in B16 metastasis-inhibited mice. Mice were injected intrasplenically with vehicle, B16 cells, or Hepa1-6 cells and then with AcMNPV 1 day later (n = 8 to 9). After 14 days, lymphocytes from mouse intestinal lymph nodes were pooled and stimulated in vitro with B16 cells as previously described (18). Cytotoxic activity was assayed after 5 days of incubation. Target cells (0.5 to 1×10^4/well) were incubated with effector cells in RPMI 1640 containing 10% fetal calf serum (total volume, 100 μl) in 96-well round-bottom microtiter plates. Cytotoxicity was detected with the CytoTox 96 nonradioactive cytotoxicity assay kit (Promega Corp., Madison, WI). Spontaneous release from target cells was less than 15% of maximum release.

CTL cytotoxicity against B16 target cells was significantly increased in B16 cell-challenged mice (10.1% ± 1.41%) compared with mice challenged with vehicle or Hepa1-6 cells (4.13% ±

* Corresponding author. Mailing address: Department of Life and Environmental Sciences and High Technology Research Center, Chiba Institute of Technology, 2-17-1 Tsudanuma, Narashino, Chiba, Japan. Phone: 81-47-478-0407. Fax: 81-47-471-8764. E-mail: hiroshi.takaku@it-chiba.ac.jp

▽ Published ahead of print on 5 December 2007.

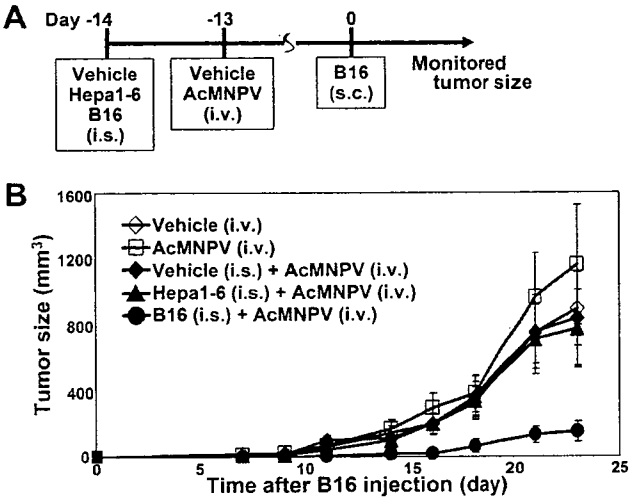

FIG. 1. Acquired immune effects of AcMNPV injection in mouse B16 melanoma tumors. (A) Schematic of the experiment. Mice were injected intrasplenically on day −14 with vehicle or with 1×10^6 B16 or Hepa1-6 cells. AcMNPV (1×10^8 PFU/mouse) was injected intravenously on day −13. After 2 weeks, the mice received a subcutaneous secondary challenge with 2×10^5 B16 cells in 0.1 ml phosphate-buffered saline. Mice were monitored every 2 to 3 days for tumor growth (B). i.v., intravenous; i.s., intrasplenic; s.c., subcutaneous. Error bars indicate standard deviations.

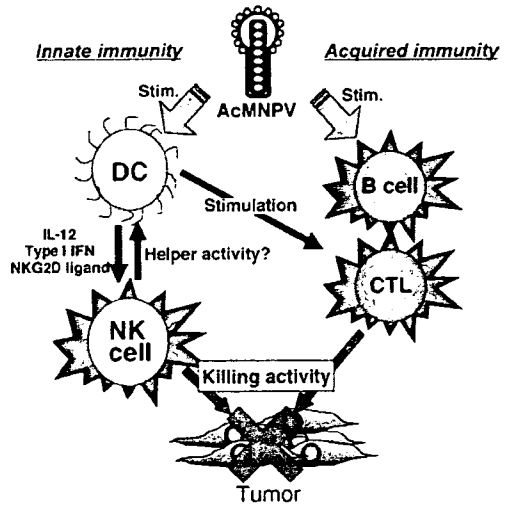

FIG. 3. Hypothetical AcMNPV-induced antitumor mechanisms in mice. AcMNPV stimulates antigen-presenting cells such as DCs and B cells. In innate immunity, cytokines and NKG2D ligands provide NK cell killing activity against tumor cells. In acquired immunity, tumor-specific CTLs and antibodies are induced.

0.81% and 4.49% ± 1.05%, respectively) at an effector/target cell ratio of 50 (Fig. 2A), indicating that AcMNPV induces B16 cell-specific CTL activity. Data were analyzed using a two-tailed Student *t* test.

Mice were injected intrasplenically with vehicle or 1×10^6 B16 cells and then with AcMNPV 1 day later. After 14 days, serum was harvested and stored at −80°C. Immunodetection using an antibody against B16 cells was performed as previously described (19). The measured B16 cell-specific absorbance of serum from AcMNPV-injected mice was significantly increased compared with that of serum from vehicle-injected mice (AcMNPV, 11.5% ± 3.9%; vehicle, 1.41% ± 0.74%) (Fig. 2B), indicating that AcMNPV increased the antibody titer against challenged tumor cells. Next, we determined whether the serum antibodies could mediate cytotoxicity against tumor cells. B16 cell-specific antibody-mediated complement-dependent cytotoxicity was determined as previously described (6). Cytotoxicity was detected with the CytoTox 96 nonradioactive cytotoxicity assay kit. B16 cell-specific cytotoxicity from the sera of AcMNPV-treated mice was significantly increased compared with that from sera of vehicle-injected mice (AcMNPV, 11.5% ± 3.9%; vehicle, 1.41% ± 0.74%) (Fig. 2C), suggesting that AcMNPV induced effective antitumor antibodies. Data were analyzed using a two-tailed Student *t* test.

Figure 3 shows a hypothetical model of AcMNPV-induced antitumor mechanisms in mice. Initially, AcMNPV induces NK cell-dependent killing activity against tumor cells through the activation of cytokines and NKG2D ligands (12). In acquired immunity, tumor-specific CTLs and antibodies are induced. Thus, these results suggest that AcMNPV induces strong antitumor effects in both innate and acquired immunity.

Most viruses currently employed for gene therapy can utilize

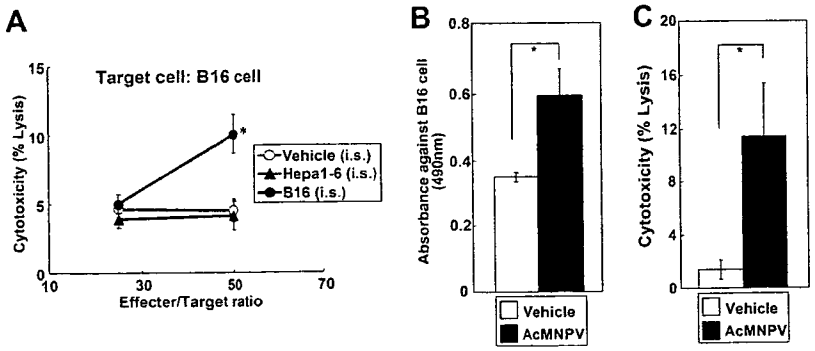

FIG. 2. Effect of AcMNPV injection on CTL activity and specific antibody titer. (A) CTL activity against B16 melanoma cells in mice intrasplenically challenged with vehicle, Hepa1-6 cells, or B16 cells challenged and treated with AcMNPV. (B) B16-specific antibody titer in serum. (C) Antibody-mediated complement-dependent cytotoxicity in serum. Data represent means ± standard deviations. *, $P < 0.05$.

humans as a host, and their replication can lead to pathogenesis and toxicity. By contrast, baculoviruses do not replicate in humans (23), instead using insects as hosts. AcMNPV has been registered as a type of insecticide with the U.S. Environmental Protection Agency (8, 22) and is used clinically in multiple protein expression systems (4, 7). Recently, it was shown that injection of B6 mice with AcMNPV did not lead to activation of hepatic enzymes, such as plasma alanine aminotransferase or aspartate aminotransferase (12). Although these observations suggest that baculovirus is potentially a safer option for applications in humans, this remains to be confirmed, and toxicity in animals must be examined prior to its use in clinical trials.

In conclusion, we have shown that wild-type AcMNPV induces antitumor acquired immunity against challenged tumor cells in the form of increased CTL activity and tumor-specific antibody production. This suggests that it could be a useful and efficient antitumor agent which induces antitumor innate and acquired immunity.

We thank Y. Shoji and Y. Tsuyama for secretarial work.

This work was supported, in part, by a Grant-in-Aid for High Technology Research (no. 09309011) from the Ministry of Education, Science, Sports, and Culture, Japan, and by a grant from the Research and Development Program for New Bio-industry Initiatives.

REFERENCES

1. **Abe, T., H. Hemmi, H. Miyamoto, K. Moriishi, S. Tamura, H. Takaku, S. Akira, and Y. Matsuura.** 2005. Involvement of the Toll-like receptor 9 signaling pathway in the induction of innate immunity by baculovirus. J. Virol. **79**:2847–2858.
2. **Abe, T., H. Takahashi, H. Hamazaki, N. Miyano-Kurosaki, Y. Matsuura, and H. Takaku.** 2003. Baculovirus induces an innate immune response and confers protection from lethal influenza virus infection in mice. J. Immunol. **171**:1133–1139.
3. **Andersen, M. H., D. Schrama, P. Thor Straten, and J. C. Becker.** 2006. Cytotoxic T cells. J. Investig. Dermatol. **126**:32–41.
4. **Ayres, M. D., S. C. Howard, J. Kuzio, M. Lopez-Ferber, and R. D. Possee.** 1994. The complete DNA sequence of Autographa californica nuclear polyhedrosis virus. Virology **202**:586–605.
5. **Berger, I., D. J. Fitzgerald, and T. J. Richmond.** 2004. Baculovirus expression system for heterologous multiprotein complexes. Nat. Biotechnol. **22**:1583–1587.
6. **Chen, H. W., Y. P. Lee, Y. F. Chung, Y. C. Shih, J. P. Tsai, M. H. Tao, and C. C. Ting.** 2003. Inducing long-term survival with lasting anti-tumor immunity in treating B cell lymphoma by a combined dendritic cell-based and hydrodynamic plasmid-encoding IL-12 gene therapy. Int. Immunol. **15**:427–435.
7. **Cheng, T., C. Y. Xu, Y. B. Wang, M. Chen, T. Wu, J. Zhang, and N. S. Xia.** 2004. A rapid and efficient method to express target genes in mammalian cells by baculovirus. World J. Gastroenterol. **10**:1612–1618.
8. **Cory, J. S., M. L. Hirst, T. Williams, R. S. Hails, D. Goulson, B. M. Green, T. M. Carty, R. D. Possee, P. J. Cayley, and D. H. L. Bishop.** 1994. Field trial of a genetically improved baculovirus insecticide. Nature **370**:138–140.
9. **Fipaldini, C., B. Bellei, and N. La Monica.** 1999. Expression of hepatitis C virus cDNA in human hepatoma cell line mediated by a hybrid baculovirus-HCV vector. Virology **255**:302–311.
10. **Gronowski, A. M., D. M. Hilbert, K. C. Sheehan, G. Garotta, and R. D. Schreiber.** 1999. Baculovirus stimulates antiviral effects in mammalian cells. J. Virol. **73**:9944–9951.
11. **Hofmann, C., V. Sandig, G. Jennings, M. Rudolph, P. Schlag, and M. Strauss.** 1995. Efficient gene transfer into human hepatocytes by baculovirus vectors. Proc. Natl. Acad. Sci. USA **92**:10099–10103.
12. **Kitajima, M., T. Abe, N. Miyano-Kurosaki, M. Taniguchi, T. Nakayama, and H. Takaku.** Baculovirus Autographa caliphornica multiple nuclear polyhedrosis virus-induced natural killer-dependent antitumor immunity. Mol. Ther., in press.
13. **Kitajima, M., H. Hamazaki, N. Miyano-Kurosaki, and H. Takaku.** 2006. Characterization of baculovirus Autographa californica multiple nuclear polyhedrosis virus infection in mammalian cells. Biochem. Biophys. Res. Commun. **343**:378–384.
14. **Liu, S. H., M. Zhang, and W. G. Zhang.** 2005. Strategies of antigen-specific T-cell-based immunotherapy for cancer. Cancer Biother. Radiopharm. **20**: 491–501.
15. Reference deleted.
16. **Matsuura, Y., R. D. Possee, H. A. Overton, and D. H. Bishop.** 1987. Baculovirus expression vectors: the requirements for high level expression of proteins, including glycoproteins. J. Gen. Virol. **68**:1233–1250.
17. **McCormick, C. J., D. J. Rowlands, and M. Harris.** 2002. Efficient delivery and regulable expression of hepatitis C virus full-length and minigenome constructs in hepatocyte-derived cell lines using baculovirus vectors. J. Gen. Virol. **83**:383–394.
18. **Okada, N., Y. Masunaga, Y. Okada, H. Mizuguchi, S. Iiyama, N. Mori, A. Sasaki, S. Nakagawa, T. Mayumi, T. Hayakawa, T. Fujita, and A. Yamamoto.** 2003. Dendritic cells transduced with gp100 gene by RGD fiber-mutant adenovirus vectors are highly efficacious in generating anti-B16BL6 melanoma immunity in mice. Gene Ther. **10**:1891–1902.
19. **Overwijk, W. W., D. S. Lee, D. R. Surman, K. R. Irvine, C. E. Touloukian, C. C. Chan, M. W. Carroll, B. Moss, S. A. Rosenberg, and N. P. Restifo.** 1999. Vaccination with a recombinant vaccinia virus encoding a "self" antigen induces autoimmune vitiligo and tumor cell destruction in mice: requirement for CD4(+) T lymphocytes. Proc. Natl. Acad. Sci. USA **96**:2982–2987.
20. Reference deleted.
21. **Song, S. U., and F. M. Boyce.** 2001. Combination treatment for osteosarcoma with baculoviral vector mediated gene therapy (p53) and chemotherapy (adriamycin). Exp. Mol. Med. **33**:46–53.
22. **Stewart, L. M., M. Hirst, M. Lopez Ferber, A. T. Merryweather, P. J. Cayley, and R. D. Possee.** 1991. Construction of an improved baculovirus insecticide containing an insect-specific toxin gene. Nature **352**:85–88.
23. **Tjia, S. T., G. M. zu Altenschildesche, and W. Doerfler.** 1983. Autographa californica nuclear polyhedrosis virus (AcNPV) DNA does not persist in mass cultures of mammalian cells. Virology **125**:107–117.

Nucleic Acids Research Advance Access published January 21, 2008

Nucleic Acids Research, 2007, 1–8
doi:10.1093/nar/gkm1043

Short-hairpin RNAs synthesized by T7 phage polymerase do not induce interferon

Takuma Gondai[1], Kazuya Yamaguchi[1], Naoko Miyano-Kurosaki[1,2], Yuichirou Habu[1,3] and Hiroshi Takaku[1,2,*]

[1]Department of Life and Environmental Science, [2]High Technology Research Center, Chiba Institute of Technology, 2-17-1 Tsudanuma, Narashino-shi, Chiba 275-0016 Japan, and [3]Japanese Foundation for AIDS Prevention, 1-3-12 Misakicho, Chiyoda, Tokyo 101-0061, Japan

Received April 5, 2007; Revised October 31, 2007; Accepted November 1, 2007

ABSTRACT

RNA interference (RNAi) mediated by small-interfering RNAs (siRNAs) is a highly effective gene-silencing mechanism with great potential for gene-therapeutic applications. siRNA agents also exert non-target-related biological effects and toxicities, including immune-system stimulation. Specifically, siRNA synthesized from the T7 RNA polymerase system triggers a potent induction of type-I interferon (IFN) in a variety of cells. Single-stranded RNA also stimulates innate cytokine responses in mammals. We found that pppGn ($n = 2,3$) associated with the 5′-end of the short-hairpin RNA (shRNA) from the T7 RNA polymerase system did not induce detectable amounts of IFN. The residual amount of guanine associated with the 5′-end and hairpin structures of the transcript was proportional to the reduction of the IFN response. Here we describe a T7 pppGn ($n = 2,3$) shRNA synthesis that does not induce the IFN response, and maintains the full efficacy of siRNA.

INTRODUCTION

RNA interference (RNAi) is a natural biological phenomenon mediated by small-interfering RNA (siRNA) molecules that target-specific messenger RNA (mRNA) for degradation by cellular enzymes. RNAi has become the method of choice for studying gene function, especially in mammalian systems. With proof-of-concept studies already reported against a wide variety of human pathogens, and several innovative methods available for delivering siRNA to a range of primary cells, there is now an even greater role for siRNA as a potential therapeutic strategy. siRNAs induce the global upregulation of interferon (IFN)-stimulated gene expression (1–4), as shown by the transfection of both enzymatically and chemically synthesized siRNAs into cells, and by siRNAs that are produced intracellularly following the expression of short-hairpin RNAs (shRNAs) (2–4). These studies documented significant non-specific changes in gene expression as a consequence of the delivery of siRNAs.

One simple method to limit the risk of inducing an IFN response is to use the lowest effective dose of the shRNA vector, as advocated by Bridge *et al.* (1). Recently, Kim *et al.* (5) demonstrated that siRNAs synthesized using the T7 RNA polymerase system trigger a potent induction of IFN-α and IFN-β in a variety of cells. The mediator of this response is an initiating 5′-triphosphate that is required for IFN induction. These findings led to the development of an improved method for bacteriophage polymerase-mediated siRNA synthesis that incorporates two 3′-adenosines to prevent base-pairing with the initiating guanines, thereby allowing RNase T1 and calf intestine alkaline phosphatase (CIP) to remove the initiating 5′-nucleotides (nt) and triphosphates of the transcripts. It is now clear that triphosphates act as triggers to induce type I IFN via the activation of retinoic acid-inducible protein I (RIG-I) (6,7). By contrast, Marques *et al.* (8) reported that blunt siRNAs are potent activators of RIG-I-mediated type I IFN induction, whereas siRNAs containing 3′-overhangs are not.

Here, we describe a new type of shRNA, pppGn(n = 2)-shRNA, synthesized by bacteriophage polymerase, which does not induce IFN. We also describe the anti-human immunodeficiency virus type 1 (HIV-1) activity of this shRNA, which targets the well-conserved dimerization initiation site (DIS) of HIV-1.

MATERIALS AND METHODS

RNAs

T7 shRNAs were synthesized using the AmpliScribe T7 High Yield Transcription Kit (Epicentre, Madison,

*To whom correspondence should be addressed: Tel: +81 47 478 0407; Fax: +81 47 471 8764; Email: hiroshi.takaku@it-chiba.ac.jp

The authors wish it to be known that, in their opinion, the first two authors should be regarded as joint First Authors.

WI) according to the manufacturer's protocol. For the *in vitro* transcription of RNA, T7 primer I (5′-TAATACGACTCACTATA-3′) was hybridized with T7 primer II, which contains the antisense sequence of each transcribed RNA, the tail sequence (5′-CCTATA GTGAGTCGTATTA-3′) and the loop sequence (5′-TC TCTTGAA-3′). For example, to make pppGG-luc3-shRNA, two primers were used (5′-TAATACGACTC ACTATA-3′) and (5′-AAGGAGCCTTCAGGATTACA AGATCTCTTGAATCTTGTAATCCTGAAGGCTCC CCTATAGTGAGTCGTATTA-3′). After a 1-h at 37°C, for the CIP, 50 U RNA (New England Biomedical, Beverly, MA) was added to the shRNA and incubated at 37°C for 1 h. Finally, the shRNAs and siRNA were purified by polyacrylamide gel electrophoresis (PAGE).

Cell culture

HeLa CD4$^+$ cells were grown in RPMI 1640 medium (Sigma Chemical Co., St Louis, MO) supplemented with 10% (v/v) heat-inactivated fetal bovine serum, 100 U/ml penicillin and 100 μg/ml streptomycin.

Assays for IFN

The amount of IFN-β secreted into the growth medium was determined using IFN ELISA kits (PBL Biomedical Laboratories, Piscataway, NJ). HeLa CD4$^+$ or RIG-I silencing HeLa CD4$^+$ cells were transfected with 100 nM shRNAs or siRNA using DMRIE-C (Invitrogen, San Diego, CA) according to the manufacturer's protocol, and were placed in 12-well plates. After 90 min, the cells were washed with RPMI-1640. Medium from RNA-transfected HeLa CD4$^+$ cells was collected 12 h later, serially diluted and assayed for the amount of secreted IFN according to the manufacturer's protocol. Each assay was performed in triplicate. Antibody neutralization assays were carried out by diluting the medium to 3.3% with fresh medium and mixing with 100 U/ml IFN-β neutralizing antibody (PBL Biomedical Laboratories) for 1 h.

Dual-luciferase reporter assay

HeLa CD4$^+$ cells in 12-well plates were co-transfected with 0.2 μg firefly luciferase vector, pGL3 control vector or pNL_{4-3}-luc, and 0.2 μg pRG-TK control vector containing Renilla luciferase (Promega Corp. Madison, WI) using FuGENE^{TM}6 (Roche Diagnostics, Basel, Switzerland) according to the manufacturer's protocol. shRNAs were used at a concentration of 12.5–50 nM per well. Firefly and Renilla luciferase activities were measured consecutively using dual-luciferase assays (Promega) 48 h after transfection.

Assay of HIV-1 replication

HIV-1 production was monitored by determining the HIV-1 p24 antigen concentration. HeLa CD4$^+$ cells were transfected with shRNAs or LacZ (control shRNA) using DEMRI-C (Invitrogen). After 90 min, the cells were washed with serum-free RPMI-1640 and then transfected with pNL_{4-3} using FuGENE^{TM}6 (Roche Diagnostics) according to the manufacturer's protocol. The culture medium from HeLa CD4$^+$ cells was harvested 2 days post-transfection. p24 Gag protein production was detected by the HIV-1 p24 chemiluminescent enzyme immunoassay (CLEIA; Lumipulse, Fujirebio Inc., Tokyo, Japan), according to the manufacturer's protocol (9).

Dual-luciferase reporter assay of IRF-3 activity

HeLa CD4$^+$ cells were seeded at a density of 1×10^5 cells per well into 12-well plates for 24 h, and then transfected with 0.5 μg pIRF-3/Luc DNA (10) and 0.2 μg phRG-TK using FuGENE^{TM}6 (Roche Diagnostics) according to the manufacturer's protocol. After 24 h, 100 nM shRNA or 0.5 μg/ml polyinosinic acid:polycytidylic acid (poly I:C) was transfected using DMRIE-C (Invitrogen). Untreated cells were used as a control. Firefly and Renilla luciferase activities were measured consecutively using dual-luciferase assays (Promega Corp.) 12 h after transfection.

MTS assay

HeLa CD4$^+$ cells (2×10^4 cells/ml) were seeded into 96-well microtitre plates and incubated in the presence of various concentrations of the test compounds. The dilutions ranged from one-fold to five-fold, and nine concentrations were examined. All of the experiments were performed in triplicate. After 3 days culture at 37°C in a CO_2 incubator, cell viability was quantified by a colorimetric assay monitoring the ability of viable cells to reduce 3-(4,5-dimethylthiazol-2-yl)-5-(3-carboxymethoxyphenyl)-2-(4-sulfophenyl)-2H-tetrazolium, inner salt (MTS; Promega Corp.) to a red formazan product (11). The absorbances were read by a microcomputer-controlled photometer (Titertec MultiscanR; Labsystem Oy, Helsinki, Finland) at a single wavelength (492 nm). These values were then translated into percentages per well.

RNA interference in HeLa CD4$^+$ cells

HeLa CD4$^+$ cells were transfected with 100 nM siRNAs targeting RIG-I (sense CGAUUCCAUCACUAUCC AUtt; antisense, AUGGAUAGUGAUGGAAUCGtt; Sigma Aldrich Japan, Hokkaido, Japan) using DMRIE-C (Invitrogen) according to the manufacturer's protocol, and were placed in 12-well plates.

Reverse-transcription polymerase chain reaction (RT-PCR)

Total cellular RNA was prepared using TRIZOL (Invitrogen). RIG-ImRNA was detected by a RT-PCR High–Plus kit (Toyobo, Kyoto, Japan) with the following specific primers: RIG-I sense, 5′-TCCTTTATGAGTAT GTGGGCA-3′; and RIG-I antisense, 5′-TCGGGCACA GAATATCTTTG-3′. Glyceraldehyde-3-phosphate dehydrogenase (GAPDH)-specific primers were used as a loading control in a separate reaction. The reaction parameters were 2 min at 94°C, followed by 40 cycles of 1 min at 94°C and 1.5 min at 60°C.

RESULTS

pppGn(n = 2)-shRNA does not induce IFN

To investigate the RNAi-mediated silencing of luciferase activity, we initially synthesized six shRNAs targeting the luciferase gene transcript using T7 RNA polymerase. The main advantages of this technique are its simplicity and low cost compared with chemical synthetic RNA (12,13). The luc-shRNAs include a 5′-pppGn (n = 2) sequence, because efficient T7 RNA polymerase initiation requires the first and second non-transcribed spacer of each RNA to be a guanine.

To determine whether pppGn(n = 2)-shRNA-luc specifically inhibited luciferase gene expression, HeLaCD4$^+$ cells were transfected with pppGn(n = 2)-shRNA-luc corresponding to the luciferase gene, and then transfected with pGL3-control (Firefly) and phRG-TK (Renilla) vectors. We found that pppGn(n = 2)-shRNA-luc3 (nt 824–845) and pppGn (n = 2)-shRNA-4 (nt 893–914) greatly inhibited luciferase activity (data not shown).

Recently, Kim *et al.* (5) demonstrated that siRNAs synthesized using the T7 RNA polymerase system trigger the potent induction of IFN-α and IFN-β in a variety of cells. The mediator of this response was an initiating 5′-triphosphate that was required for IFN induction. To verify the induction of IFN by pppGn(n = 2)-shRNA-luc3, we designed pppGn (n = 0–3) in association with the 5′-end of shRNA-luc3, which was transcribed by T7 RNA polymerase (Figure 1A). Luc-3 inhibited luciferase activity in a dose-dependent manner (Figure 1B). The control pppGn(n = 2)-shRNA-EGFP targeting enhanced green fluorescent protein did not inhibit luciferase activity (Figure 1B). Furthermore, the inhibition of luciferase activity was not due to the residual amount of guanine associated with the 5′-end of the transcript.

We also designed 5′-HOGn(n = 0–3)-luc-3 with the 5′-end of shRNA and tested for IFN induction (Figure 1A). We assayed the medium of pppGn or 5′-HOGn(n = 0–3)-shRNA-luc3-transfected HeLa CD4$^+$ cells for IFN-β using an enzyme-linked immunosorbent assay (ELISA). IFN assays from pppGn (n = 2,3) associated with the 5′-end of shRNA did not induce IFN in HeLa CD4$^+$ cells (Figure 2A), whereas a slight IFN response was induced by pppGn (n = 1) associated with the 5′-end of shRNA. pppGn (n = 0) associated with the shRNA 5′-end was capable of more potent IFN induction than pppGn (n = 1) associated with the shRNA 5′-end. Furthermore, no IFN was induced in HeLa CD4$^+$ cells by 5′-HOGn (n = 0–3) (Figure 2A).

To further investigate the pppGn(n = 0–3)-shRNA-luc3-mediated or 5′-HOGn(n = 0–3)-shRNA-luc3-mediated IFN response, we monitored cell growth. pppGn(n = 0)-shRNA-luc3-transfected cells showed a cytopathogenic effect after 3 d, but pppGn(n = 2,3)-shRNA-luc3-transfected cells did not (Figure 2B). A tetrazolium-based MTS assay was next used to examine the viability of pppGn(n = 0–3)-shRNA-luc3-transfected or 5′-HOGn(0–3)-shRNA-luc3-transfected cells. pppGn (n = 2,3) associated with the shRNA 5′-end or 5′-HOGn(0–3)-shRNA-luc3 did not induce cellular toxicity

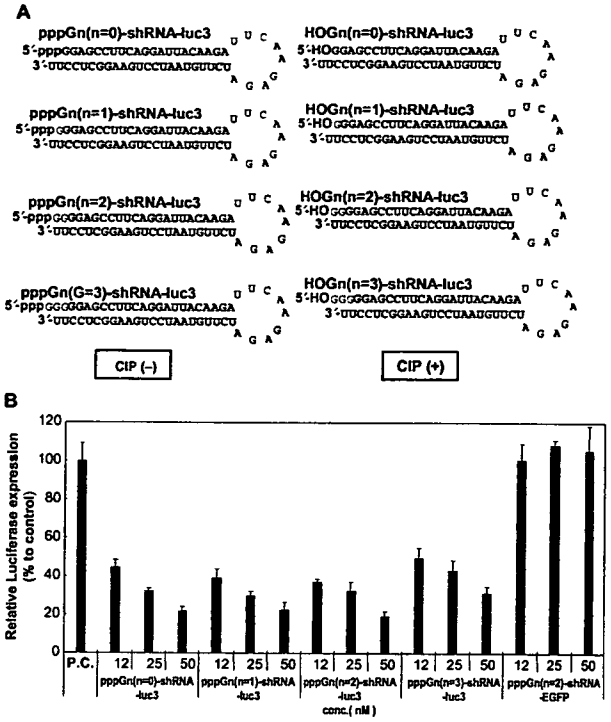

Figure 1. RNAi-mediated silencing of luciferase activity. (A) The shRNA-luc synthesized in these studies. We designed pppGn (n = 0–3) associated with the 5′-end of the shRNA that was transcribed by T7 RNA polymerase. We also designed 5′-HOGn (n = 0–3) with the 5′-end of the shRNA (removal of triphosphate by CIP). (B) The anti-luciferase activity of pppGn (n = 0–3) associated with the 5′-end of shRNA-luc3 in HeLaCD4$^+$ cells. Firefly and Renilla luciferase activities were measured consecutively using dual-luciferase assays (Promega) 48 h after transfection. The average results of three independent experiments are presented.

in HeLa CD4$^+$ cells (Figure 2C), whereas minor cellular toxicity was induced by pppGn(n = 0,1)-shRNA-luc3.

The antiviral activities of IFN have been recently studied (14), but our data indicate that the presence of a guanine residue on T7-transcribed RNAs prevents the activation of IFN. Furthermore, the inhibition of luciferase activity by pppGn(n = 0)-shRNA-luc3 (Figure 2A–C) might be due, in part, to IFN induction. These results suggest that the residual amount of guanine associated with the 5′-end of the transcript is proportional to the reduction of the IFN response.

Inhibition of HIV-1 replication by shRNAs synthesized using T7 RNA polymerase

To confirm the role of residual guanine, we tested the sequence-specific inhibition of HIV-1 replication by shRNAs synthesized using the T7 RNA polymerase. We applied the shRNA technology to a well-conserved target in HIV-1: the dimerization initiation site (DIS) (15,16). The DIS is a stem–loop structure with six self-complementary nt at the top (Figure 3A), which is located between the primer binding site and the splice donor site at the end of a long terminal repeat (LTR) (17). It is involved

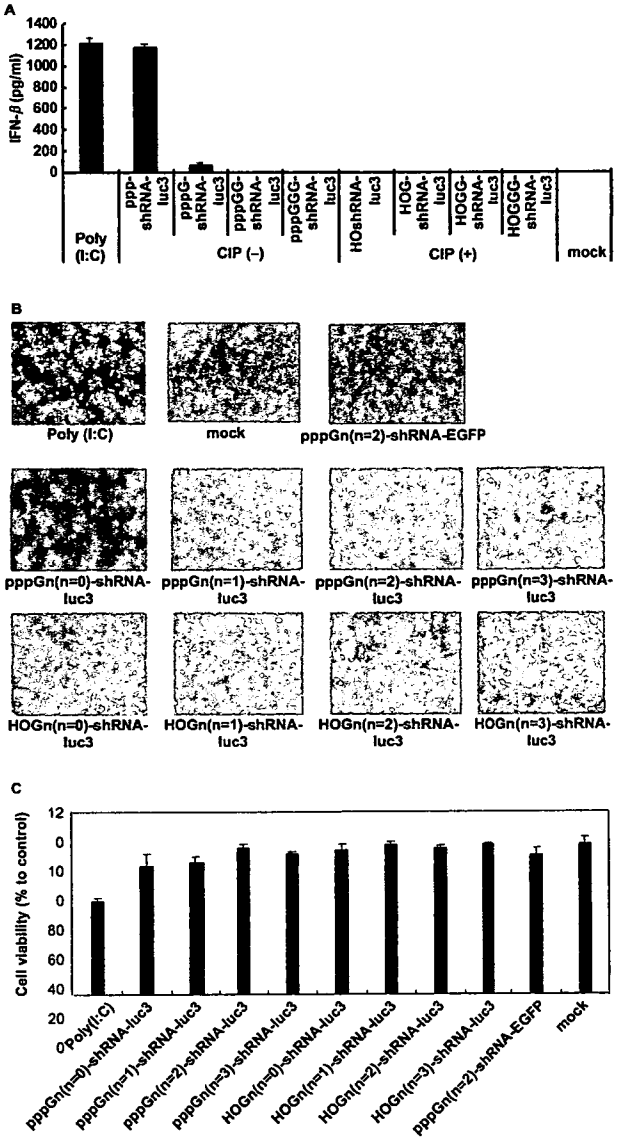

Figure 2. Lack of IFN induction by T7-transcribed shRNA. (**A**) The residual amount of guanine associated with the 5′-end of the transcript is essential to prevent IFN induction. HeLaCD4$^+$ cells were transfected with 100 nM of pppGn(n = 0–3)-shRNA-luc3 or HOGn(n = 0–3)-shRNA-luc3. The induced levels of IFN-β were determined by an ELISA. The IFN results are the average of two independent experiments. (**B**) The cytopathic effect of T7-transcribed pppGn(n = 0–3)-shRNA-luc3. HeLaCD4$^+$ cells were transfected with 100 nM of pppGn(n = 0–3)-shRNA-luc3 or HOGn(n = 0–3)-shRNA-luc3 and monitored microscopically 3 days post-transfection. (**C**) Cytotoxicity of pppGn(n = 0–3)-shRNA-luc3 (100 nM) or HOGn(n = 0–3)-shRNA-luc3 (100 nM) represents the percentage reduction of viable cell numbers in HeLaCD4$^+$ cells. The cytotoxicity assay was performed with an MTS assay. The toxicity results are representative of three independent experiments.

in the dimerization of the HIV-1 genome, packaging and proviral synthesis (18–22). There are two major motifs in HIV-1: GUGCAC in subtypes A and C, and GCGCGC in subtypes B and D (23,24). The subtype A motif has been shown to be a good siRNA target in an *in vitro* cell-free system where HIV-1 genome dimerization was successfully inhibited by a 9-mer DIS-targeting siRNA, while the corresponding DNA oligonucleotide did not affect dimerization (25,26). These studies also showed that sense oligonucleotides function as competitive inhibitors of this self-complimentary target.

pppGn(n = 2)-shRNA-DIS (shRNA-DIS-1-8) targeted against the 35-nt stem-loop (nt 248–277) or the 9-nt loop of the DIS (nt 255–263) were tested for their ability to inhibit HIV-1 replication (Figure 3B). The effect of shRNA-DIS-1-8 on HIV-1 (pNL$_{4\text{-}3}$-luc) (27) replication was measured in a transient assay following its co-transfection with pNL$_{4\text{-}3}$-luc into HeLa CD4$^+$ cells. At 48 h post-transfection, luciferase activity was measured with the dual-luciferase reporter (DLR^{TM}) assay system. The luciferase activity of the cell lysate was measured as an indirect marker of viral replication. Although shRNA-DIS-3, shRNA-DIS-7 and shRNA-DIS-8 had strong inhibitory effects compared with shRNA-DIS-1 and shRNA-DIS-2, their anti-HIV-1 activities were lower than those of shRNA-DIS-4, shRNA-DIS-5 and shRNA-DIS-6 (Figure 3C). The internal control, pppGn(n = 2)-shRNA-LacZ targeting LacZ protein, did not inhibit luciferase activity.

Sequence-specific inhibition of HIV-1 replication by T7 transcribed shRNA-DIS-6

To further investigate the specific effect of shRNA-DIS6 on the DIS sequence, we examined shRNA-DIS-6 and the internal control shRNA-LacZ against infection by HIV-1$_{NL4\text{-}3}$ (Figure 4A). The shRNA-DIS effect was confirmed as specific to the DIS gene, because no obvious effects were observed following the HIV-1$_{NL4\text{-}3}$ challenge.

We next carried out an IFN-β ELISA assay of the medium of pppGn(n = 2)-shRNA-DIS6-transfected, HOGn(n = 0)-shRNA-DIS6-transfected, and ppp Gn(n = 2)-shRNA-LacZ-transfected HeLa CD4$^+$ cells, and found no IFN induction (Figure 4B). By contrast, pppGn (n = 0) associated with the shRNA 5′-end induced IFN. Kim *et al.* (5) reported that the pppGGG-dsRNA (such as small interfering RNA), when generated by *in vitro* transcription, induced IFN. We examined the influence of pppGGG associated with short dsRNA [pppGn(n = 2)-siRNA-DIS6] on IFN inducing activity. When HeLa CD4$^+$ cells were transfected with pppGn(n = 2)-siRNA-DIS6, we observed IFN induction, but not the pppGn(n = 2)-shRNA-DIS6 (Figure 4B). Our result on the induce of IFN by pppGn(n = 2)-siRNA-DIS6 was in general agreement with their IFN response as reported by Kim *et al.* (5). To further clarify the IFN response of pppGn (n = 0,2) in association with the shRNA 5′-end, we examined the activation of IFN-regulatory factor-3 (IRF-3) in HeLa CD4$^+$ cells. We assessed the trigger of IRF-3 phosphorylation by pppGn(n = 0,2)-shRNA-DIS6 and HOGn(n = 0)-shRNA-DIS6 in HeLa CD4$^+$ cells by constructing a luciferase reporter gene-expression vector (pIRF-3/Luc reporter) with an IRF-3 binding region (5′-GAAACCGA AACT-3′) in the pGL3-basic vector (28). pIRF-3/Luc and

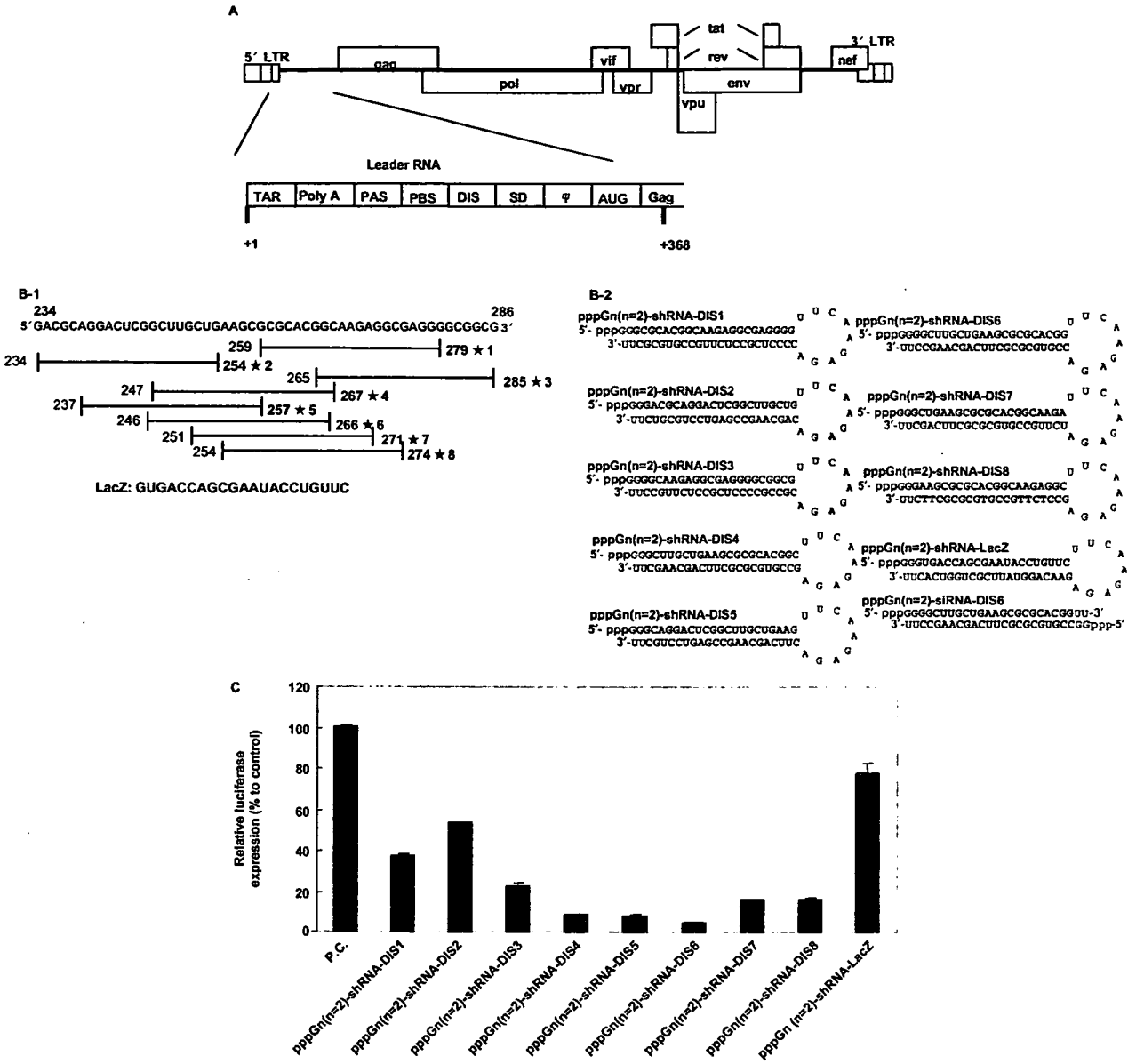

Figure 3. Inhibition of HIV-1 replication by shRNAs synthesized using T7 RNA polymerase. (**A**) Schematic of the 9.2-kb HIV genome. The 5′-LTRs and 3′-LTRs and all eight open-reading frames are indicated. The untranslated leader RNA consists of several regulatory domains. (**B**) shRNAs or siRNA targeted against the DIS of HIV-I RNA (nt 248–277). (**C**) The effect of shRNA-DIS1-8 on HIV-1 (pNL_{4-3}-luc) replication was measured in a transient assay following its co-transfection with pNL_{4-3}-luc into HeLa CD4$^+$ cells. Firefly and Renilla luciferase activities were measured consecutively using dual-luciferase assays (Promega) 48 h after transfection. The luciferase activity of the cell lysate was measured as an indirect marker of viral replication. The average results of three independent experiments are presented.

pppGn(n = 0,2)-shRNA-DIS-6 were then co-transfected into HeLa CD4$^+$ cells. IRF-3 activation was monitored using the DLR^{TM} assay (Figure 4C). The internal control, polyI:C and pppGn(n = 0)-shRNA-DIS6 simultaneously induced phosphorylation of IRF-3 and luciferase gene expression in HeLa CD4$^+$ cells. By contrast, pppGn(n = 2)-shRNA-DIS6 and HOGn(n = 0)-shRNA-DIS6 did not mediate either IRF-3 phosphorylation or luciferase gene expression in these cells (Figure 4C). To further clarify the RIG-I-mediated IFN response to pppGn(n = 0,2)-shRNA, we used RNAi to specifically target RIG-I in HeLa CD4$^+$ cells. After 2 days, cells were transfected with shRNAs [pppGn (n = 0,2) or HOGn(n = 0)-shRNA-DIS6] using DMRIE-C, and the IFN ELISA assay were carried out. However, pppGn (n = 0,2)-shRNA-DIS6 and HOGn(n = 0)-shRNA-DIS6 strongly inhibited INF-β production (Figure 4D). These data indicate that pppGn(n = 0)-shRNA induced an

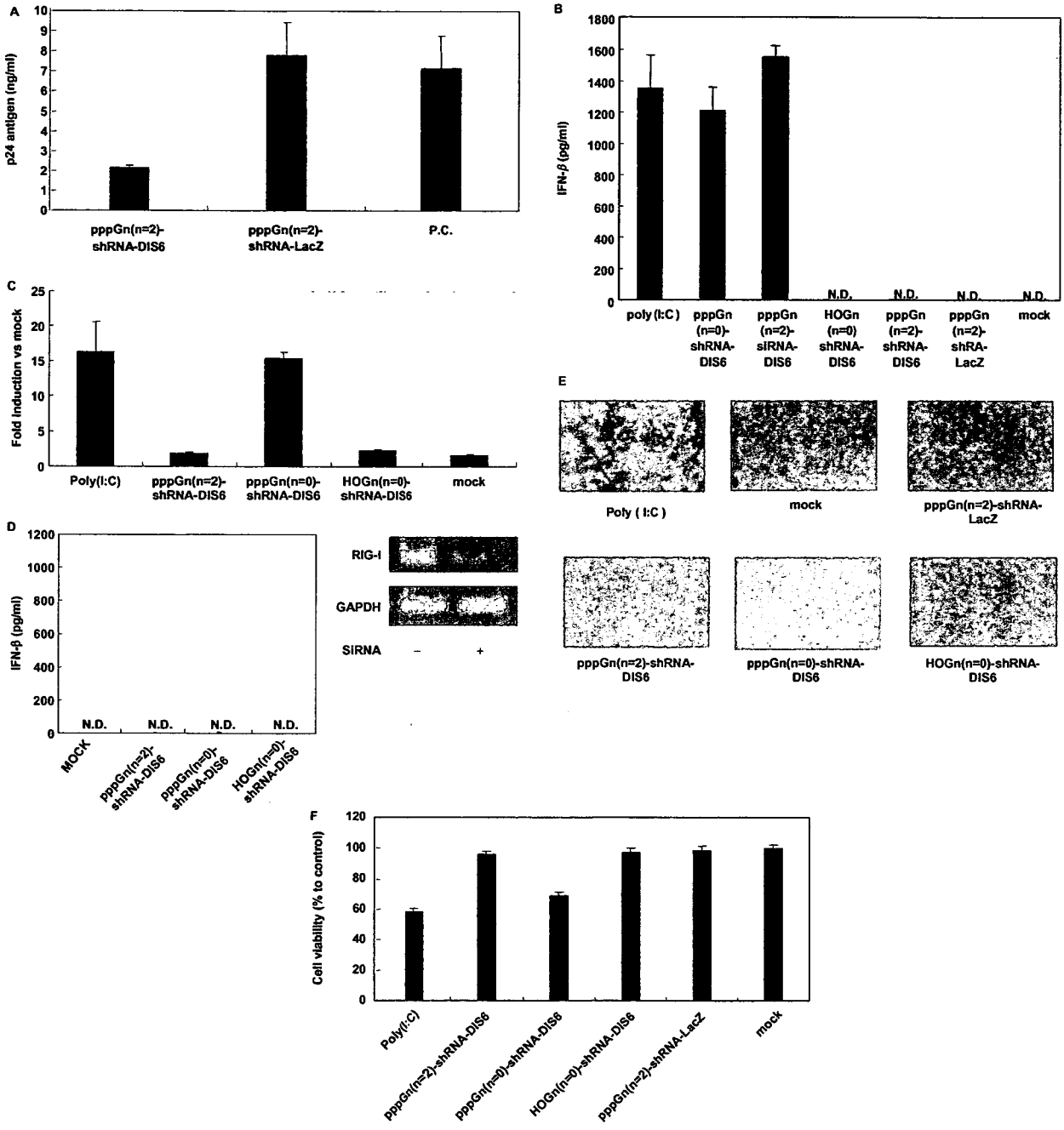

Figure 4. Sequence-specific inhibition of HIV-1 replication by T7-transcribed shRNA-DIS-6. (**A**) T7-transcribed pppGn(n = 2)-shRNA-DIS6 and LacZ (control) against challenge infection of HIV-1_{NL4-3}. The average results of three independent experiments are presented. (**B**) The residual amount of guanine associated with the 5′-end of the transcript is essential to prevent the induction of IFN. HeLaCD4$^+$ cells were transfected with 100 nM of either pppGn(n = 0,2)-shRNA-DIS6, HOGn(n = 0)-shRNA-DIS6 and pppGn(n = 2)-shRNA-LacZ (control) or pppGn(n = 2)-siRNA-DIS6 (control). The induced levels of IFN-β was determined by an ELISA. ND, not detectable. The IFN results are the average of two independent experiments. (**C**) Activation of IRF-3 by T7-transcribed shRNA. HeLaCD4$^+$ cells transfected with pIRF-3/Luc plasmid and Renilla luciferase control plasmids were either pppGn(n = 0,2)-shRNA-DIS6 and HOGn(n = 0)-shRNA-DIS6. After 12 h, the cell lysates were prepared and assayed for dual luciferase activity. The average results of three independent experiments are presented. (**D**) RIG-I siRNA inhibited the IFN-β response by pppGn(n = 0,2)-shRNA-DIS6 or HOGn(n = 0)-shRNA-DIS6. HeLaCD4$^+$ cells were transfected with siRNA targeting RIG-I. After 2 d, HeLaCD4$^+$ cells were transfected with 100 nM of either pppGn(n = 0,2)-shRNA-DIS6 or HOGn(n = 0)-shRNA-DIS6. The induced levels of IFN-β were determined by an ELISA. N.D., not detectable. The IFN results are the average of three independent experiments. (**E**) Cytotoxic effect of T7-transcribed pppGn(n = 2)-shRNA-DIS6 or pppGn(n = 2)-shRNA-LacZ. HeLaCD4$^+$ cells were transfected with pppGn(n = 2)-shRNA-DIS6 or pppGn(n = 2)-shRNA-LacZ (control) and monitored microscopically 3 days post-transfection. (**F**) The cytotoxicity of pppGn(n = 0,2)-shRNA-DIS-6 or HOGn(n = 2)-shRNA-DIS6 represented as the percentage reduction of viable HeLaCD4$^+$ cells. A cytotoxicity assay was performed along with an MTS assay. The toxicity results are representative of the three independent experiments.

RIG-I-mediated INF response, whereas pppGn(n = 2)-shRNA arrested INF-inducing activity through TLR-3 and RIG-I.

We next monitored cell growth. The pppGn(n = 0)-shRNA-DIS6-transfected cells showed cytopathogenic effects after 3 days, but the pppGn(n = 2)-shRNA-DIS6-transfected cells did not (Figure 4E). Finally, we used the MTS assay to examine the viability of pppGn(n = 0,2)-shRNA-DIS-6-transfected HeLa $CD4^+$ cells. HOGn (n = 2)-shRNA-DIS-6 and pppGn(n = 2)-shRNA-DIS-6 or LacZ did not induce cellular toxicity (Figure 4E), whereas control polyI:C and pppGn(n = 0)-shRNA-DIS-6 did (Figure 4F). Together, these data indicate that the residual guanine associated with the 5′-end and the hairpin-loop structures of the transcript is proportional to the reduction of the IFN response.

DISCUSSION

The present study demonstrates that the previously proposed scheme of triphosphate-dependent siRNA recognition (5) is, in fact, reversed; although T7-transcribed-siRNA induced a vigorous type I IFN response, 5′OH-siRNA did not.

Our studies raise the question of how the residual guanine that is associated with the 5′-end of the transcript contributes to reducing the IFN response. To investigate the RNAi-mediated silencing of luciferase activity, we synthesized shRNA-luc, including the 5′-pppGn (n = 0–3) sequence, because efficient T7 RNA polymerase initiation requires the first and second non-transcribed space of each RNA to be a guanine. The pppGn (n = 2,3) associated with the 5′-end of shRNA does not induce IFN in HeLa $CD4^+$ cells (Figure 2A), whereas the IFN response was weakly initiated by the pppGn (n = 1) associated with the 5′-end of the shRNA. The pppGn (n = 0) associated with the 5′-end of the shRNA more potently induced IFN than the pppGn (n = 1) associated with the 5′-end of the shRNA. Furthermore, 5′-HOGn (n = 0–3) did not induce IFN in HeLa $CD4^+$ cells. Our results suggest that the residual amount of guanine associated with the 5′-end of the transcript is proportional to the reduction of the IFN response. In another study, T7-transcribed siRNAs triggered a potent induction of IFN-α and IFN-β in a variety of cells, and the mediator of this response was an initiating 5′-triphosphate that was required for IFN induction (5). More recently, two groups reported that type I IFN is induced by the activation of RIG-I by 5′-triphosphate RNA (6,7). It will be important to re-examine these data in light of the possibility that these RNAs contain triphosphates, which complicates the interpretation. Our data indicate that 5′-triphosphates are responsible for inducing IFN activity, whereas the residual amount of guanine associated with the 5′-end of the transcript arrests the IFN response. To reconfirm the role of the residual amount of guanine associated with the 5′-end of the shRNA, we tested the sequence-specific inhibition of HIV-1 replication by shRNAs synthesized using T7 RNA polymerase. The HIV genome is a homodimer of two sense RNA single strands. We applied the shRNA technology to a well-conserved target in HIV-1, the DIS (15,16). The pppGn(n = 2)-shRNA-DIS6, as the target of the DIS gene, was a more potent inhibitor than the other types of shRNA-DIS. The synthesized pppGn(n = 2)-shRNA-DIS6 did not induce the activation of IFN (Figure 4B), but not the pppGn(n = 0)-shRNA-DIS6 and pppGn(n = 2)-siRNA-DIS6. Furthermore, the activation of IRF-3 did not induce with the pppGn(n = 2)-shRNA-DIS6 and HOGn(n = 0)-shRNA-DIS6, but not the pppGn(n = 0)-shRNA-DIS6 (Figure 4C). However, RIG-I-siRNA transfected cells which did not stimulation of IFN by both pppGn (n = 0) or pppGn(n = 2)-shRNA-DIS6 (Figure 4D). Recently, it was demonstrated that the pppGGG associated with short double-stranded RNA (dsRNA; pppGGG-dsRNA) is recognized by RIG-I but not TLR-3 (5,6). In contrast, the pppGn(n = 2)-shRNA-DIS6 also included pppGGG on the 5′-end of the shRNA, but did not recognize TLR-3 and RIG-I (Figure 4B–D). Furthermore, pppGn(n = 2)-shRNA-DIS6 presented a hairpin-loop structure together with the 5′-pppGGG, but not the presence on pppGGG-dsRNA. Hence, the pppGGG dsRNA was capable of inducing IFN (5,6), but the pppGn(n = 2)-shRNA-DIS6 with the guanine associated with the 5′-end and the hairpin-loop structures precluded the IFN response. One study suggested that synthetic short dsRNA with blunt ends is recognized by RIG-I, and that 2-nt overhangs at the 3′-end block this recognition (7). Taken together, these data indicate that the mechanism of inducing IFN by dsRNA with 5′-pppGGG can differentiate between dsRNAs with or without the guanine associated with the 5′-end and hairpin-loop structures. These results demonstrated an association with sequence-specific inhibition via the RNAi mechanism.

In conclusion, shRNAs transcribed by T7 RNA polymerase activate cells of the immune system cells and induce IFN production. However, the presence of a triphosphate on *in vitro*-transcribed RNAs can induce activation of the immune system (5). The pppGn (n = 2–3) associated with the 5′-end of the shRNA from T7 RNA polymerase did not induce detectable IFN, whereas pppGn (n = 0,1) associated with the 5′-end of the shRNA did induce IFN. Importantly, the residual amount of guanine associated with the 5′-end and the hairpin-loop structures of the transcript was proportional to the reduction of the IFN response. The improved method of T7 RNA polymerase-mediated shRNA synthesis did not require RNase treatment to remove the initiating 5′-nt and triphosphates of the transcripts. Our identification of a putative immunostimulatory motif with shRNAs provides a basis for the rational design of synthetic shRNAs that avoid inducing an immune response. This finding will help to reduce the potential for off-target gene effects.

ACKNOWLEDGEMENTS

We wish to thank Dr H. Hamazaki (Chiba Institute of Technology) for their help with IFN assay. We wish to thank Dr Kahoko Hashimoto for helpful discussions. This work

was supported by a Grant-in-Aid for High Technology Research (HTR) from the Ministry of Education, Science, Sports, and Culture, Japan, by research grants from the Human Science Foundation (HIV-K-14719), by a Grant-in-Aid for AIDS research from the Ministry of Health, Labor, and Welfare, Japan (H17-AIDS-002), and by the Sasakawa Scientific Research Grant from The Japan Science Society. Funding to pay the Open Access publication charges for this article was provided by Ministry of Health, Labor, and Welfare, Japan.

Conflict of interest statement. None declared.

REFERENCES

1. Bridge,A.J., Pebernard,S., Ducraux,A., Nicoulaz,A.L. and Iggo,R. (2003) Induction of an interferon response by RNAi vectors in mammalian cells. *Nat. Genet.*, **34**, 263–264.
2. Sledz,C.A., Holko,M., de Veer,M.J., Silverman,R.H. and Williams,B.R. (2003) Activation of the interferon system by short-interfering RNAs. *Nat. Cell Biol.*, **9**, 834–839.
3. Kariko,K., Bhuyan,P., Capodici,J. and Weissman,D. (2004) Small interfering RNAs mediate sequence-independent gene suppression and induce immune activation by signaling through toll-like receptor 3. *J. Immunol.*, **172**, 6545–6549.
4. Persengiev,S.P., Zhu,X. and Green,M.R. (2004) Nonspecific, concentration-dependent stimulation and repression of mammalian gene expression by small interfering RNAs (siRNAs). *RNA*, **10**, 12–18.
5. Kim,D.H., Longo,M., Han,Y., Lundberg,P., Cantin,E. and Rossi,J.J. (2004) Interferon induction by siRNAs and ssRNAs synthesized by phage polymerase. *Nat. Biotechnol.*, **22**, 321–325.
6. Hornung,V. *et al.* (2006) 5′-triphosphate RNA is the ligand for RIG-I. *Science*, **314**, 994–997.
7. Pichlmair,A., Schulz,O., Tan,C.P., Naslund,T.I., Liljestrom,P., Weber,F. and Reis e Sousa,C. (2006) RIG-I-mediated antiviral responses to single-stranded RNA bearing 5′-phosphates. *Science*, **314**, 997–1001.
8. Marques,J.T., Devosse,T., Wang,D., Zamanian-Daryoush,M., Serbinowski,P., Hartmann,R., Fujita,T., Behlke,M.A. and Williams,B.R. (2006) A structural basis for discriminating between self and nonself double-stranded RNAs in mammalian cells. *Nat. Biotechnol.*, **24**, 559–565.
9. Sakai,A., Hirabayashi,Y., Aizawa,S., Tanaka,M., Ida,S. and Oka,S. (1994) Investigation of a new p24 antigen detection system by the chemiluminescence-enzyme-immuno-assay. *J. Jpn. Assoc. Infect. Dis.*, **73**, 205–212.
10. Hamazaki,H., Ujino,S., Miyano-Kurosaki,N., Shimotohno,K. and Takaku,H. (2006) Inhibition of hepatitis C virus RNA replication by short hairpin RNA synthesized by T7 RNA polymerase in hepatitis C virus subgenomic replicons. *Biochem. Biophys. Res. Commun.*, **343**, 988–994.
11. Cory,A.H., Owen,T.C., Barltrop,J.A. and Cory,J.G. (1991) Use of an aqueous soluble tetrazolium/formazan assay for cell growth assays in culture. *Cancer Commun.*, **3**, 207–212.
12. Sohail,M., Doran,G., Riedemann,J., Macaulay,V. and Southern,E.M. (2003) A simple and cost-effective method for producing small interfering RNAs with high efficacy. *Nucleic Acids Res.*, **31**, e38.
13. Donze,O. and Picard,D. (2002) RNA interference in mammalian cells using siRNAs synthesized with T7 RNA polymerase. *Nucleic Acids Res.*, **30**, e46.
14. Samuel,C.E. (2001) Antiviral actions of interferons. *Clin. Microbiol. Rev.*, **14**, 778–809.
15. Paillart,J.C., Shchu-Xhilaga,M., Marquet,R. and Mak,J. (2004) Dimerization of retroviral RNA genomes: an inseparable pair. *Nat. Rev. Microbiol.*, **2**, 461–472.
16. Jakobsen,M.R., Damgaard,C.K., Andersen,E.S., Podhajska,A. and Kjems,J (2004) A genomic selection strategy to identify accessible and dimerization blocking targets in the 5′-UTR of HIV-1 RNA. *Nucleic Acids Res.*, **32**, e67.
17. Laughrea,M., Jette,L., Mak,J., Kleiman,L., Liang,C. and Wainberg,M.A. (1997) Mutations in the kissing-loop hairpin of human immunodeficiency virus type 1 reduce viral infectivity as well as genomic RNA packaging and dimerization. *J. Virol.*, **71**, 3397–3406.
18. St. Louis,D., Gotte,D., Sanders-Buell,E., Ritchey,D.W., Salminen,M.O., Carr,J.K. and McCutchan,F.E. (1998) Infectious molecular clones with the nonhomologous dimer initiation sequences found in different subtypes of human immunodeficiency virus type 1 can recombine and initiate a spreading infection in vitro. *J. Virol.*, **72**, 3991–3998.
19. Skripkin,E., Paillart,J.C., Marquet,R., Ehresmann,B. and Ehresmann,C. (1994) Identification of the primary site of the human immunodeficiency virus type 1 RNA dimerization in vitro. *Proc. Natl. Acad. Sci. USA*, **91**, 4945–4949.
20. Shen,N., Jette,L., Liang,C., Wainberg,M.A. and Laughrea,M. (2000) Impact of human immunodeficiency virus type 1 RNA dimerization on viral infectivity and of stem-loop B on RNA dimerization and reverse transcription and dissociation of dimerization from packaging. *J. Virol.*, **74**, 5729–5735.
21. McBride,M.S. and Panganiban,A.T. (1996) The human immunodeficiency virus type 1 encapsidation site is a multipartite RNA element composed of functional hairpin structures,. *J. Virol.*, **70**, 2963–2973.
22. Paillart,J.-C., Berthoux,L., Ottmann,M., Darlix,J.L., Marquet,R., Ehresmann,B. and Ehresmann,C. (1996) A dual role of the putative RNA dimerization initiation site of human immunodeficiency virus type 1 in genomic RNA packaging and proviral DNA synthesis. *J. Virol.*, **70**, 8348–8354.
23. Clever,J.L. and Parslow,T.G. (1997) Mutant human immunodeficiency virus type 1 genomes with defects in RNA dimerization or encapsidation. *J. Virol.*, **71**, 3407–3414.
24. Berkhout,B. and van Wamel,J.L. (1996) Role of the DIS hairpin in replication of human immunodeficiency virus type 1. *J. Virol.*, **70**, 6723–6732.
25. Skripkin,E., Paillart,J.C., Marquet,R., Blumenfeld,M., Ehresmann,B. and Ehresmann,C. (1996) Mechanisms of inhibition of in vitro dimerization of HIV type 1 by sense and antisense oligonucleotides. *J. Biol. Chem.*, **271**, 28812–28817.
26. Lodmell,J.S., Paillart,J.C., Mignot,D., Ehresmann,B., Ehresmann,C. and Marquet,R. (1998) Oligonucleotide-mediated inhibition of genomic RNA dimerization of HIV-1 strains MAL and LAI: a comparative analysis. *Antisense Nucleic Acid Drug Dev.*, **8**, 517–529.
27. Akkina,R.K., Walton,R.M., Chen,M.L., Li,Q.X., Planelles,V. and Chen,I.S. (1996) High-efficiency gene transfer into $CD34^+$ cells with a human immunodeficiency virus type 1-based retroviral vector pseudotyped with vesicular stomatitis virus envelope glycoprotein G. *J. Virol.*, **70**, 2581–2585.
28. Lin,R., Genin,P., Mamane,Y. and Hiscott,J. (2000) Selective DNA binding and association with the CREB binding protein coactivator contribute to differential activation of alpha/beta interferon genes by interferon regulatory factors 3 and 7. *Mol. Cell. Biol.*, **20**, 6342–6353.